DESIGN OF MICROHEATER FOR MEMS BASED GAS SENSOR

Dissertation submitted

in partial fulfillment of the requirement for the award of degree

MASTER OF ENGINEERING

in

ELECTRONICS AND COMMUNICATION

Submitted by

Palakkumar Bhatt

Roll No.: 801061019

Under supervision of

Dr. Anil Arora

Assistant Processor, ECE Department

ELECTRONICS AND COMMUNICATION

ENGINEERING DEPARTMENT

THAPAR UNIVERSITY, PATIALA-147004 (PUNJAB), INDIA

(Established under the section 3 of UGC Act, 1956)

June-2014

DECLARATION

I hereby declare that the work, which is being presented in the report, entitled "**DESIGN OF MICROHEATER FOR MEMS BASED GAS SENSOR**", in partial fulfillment of the requirements for the award of degree of Master of Engineering in Electronics and Communication submitted in Electronics and Communication Engineering Department of Thapar University, Patiala which is authentic record of my own work carried out under the guidance of **Dr. Anil Arora (Assistant Professor)**, Electronics and Communication Department during the fourth semester, June, 2014.

The matter presented in this thesis has not been submitted in any other University/Institute for the award of Master of Engineering.

Date: 30-06-2014

P Bhatt

.....

Palakkumar Bhatt

Roll No.: 801061019

This is to certify that the above statement made by the student is correct to the best of my knowledge and belief.

Date: 30-06-2014

28/6/14

.....

Dr. Anil Arora

Supervisor

Dr. Sanjay Sharma

Professor and Head, ECED

Thapar University, Patiala.

Dr. S. K. Mohapatra

Dean of Academic Affair,

Thapar University, Patiala.

ACKNOWLEDGEMENT

I would like to give special thanks to my guide **Dr. Anil Arora** (Assistant Professor) ECED, Thapar University, Patiala, for his valuable advice and splendid supervision. It has been a great honour to work under his guidance. It was his valuable discussions and endless endeavors through which I gained a lot. His constant encouragement and confidence-imbibing attitude has always been a moral support for me.

I am thankful to **Dr. Sanjay Sharma**, Professor and Head, Electronics and communication Engineering Department, for providing us with adequate infrastructure in carrying the work.

I am also thankful to **Dr. Kulbir Singh** P.G. Coordinator, Electronics and communication Engineering Department for the motivation and inspiration that triggered me for the report work.

I am greatly indebted to all of my friends who constantly encouraged me and also I would like to thank all the faculty members of ECED for the full support of my work. I am also thankful to the authors whose work have been consulted and quoted in this thesis. I thank all those who have contributed directly or indirectly to this work.

Lastly, I would like to thank my family for their years of unyielding love and for constant support and encouragement. They have always wanted the best for me and I admire their determination and sacrifice.

Palakkumar Bhatt

ABSTRACT

We introduce design of micro heater for MEMS based gas sensor for detection various gases in the surrounding environment. MEMS based gas sensors are widely used as they have several advantages like, higher performance, smaller size, ruggedness, low power consumption and low cost. Also metal oxide based sensing surfaces are used with their enormous benefits such as very low cost, high sensitivity, fast response/recovery time, simple electronic interface, ease of use, low maintenance and ability to detect large number of gases. Metal oxide sensor which uses electron depleted surface, either oxidation or reduction process occur on depleted sensing surface (oxide surface) while detection of hazardous gases. In these process electrons are added or extracted depending on metal oxide sensor whether is n-type or p-type. These processes change electrical properties of sensing surface. For oxidation and reduction processes, we need to have high temperature and this can be achieved by placing micro heater below the metal oxide sensing surface.

Micro-Heaters have been the subject of great interest owing to their extensive applications in gas sensors, humidity sensors and other micro-systems. A micro-heater should have high temperature to desired level, low power consumption and better temperature uniformity. My work is to geometric optimization of the micro-heater structure to achieve temperature uniformity. Also to compare parameters like, current density distribution, resistance, power consumption and transient temperature response for Poly-Si and Platinum based micro-heater. Different geometries are simulated using COMSOL Multiphysics 4.3 to find out best micro-heater geometry i.e. modified spiral geometry which gives better temperature uniformity. Also effect of voltage variation on temperature and dimensions variation on temperature are simulated and analyzed for Poly-Si and Platinum based micro-heater. After simulations and analysis, conclusion is made by parameters comparison to reach best solution among Poly-Si and Platinum based micro-heaters.

TABLE OF CONTENTS

LIST OF FIGURES

LIST OF TABLES

CHAPTER-1

1.1 Introduction

In 21st century, there is growing interest to minimize the size and the power consumption of any electronic device. There are many technologies introduced but the most optimistic technology is identified as MEMS.

1.1.1 MEMS: An Introduction

MEMS is known as Micro Electro Mechanical System. It is also known as micro system technology (MST) in Europe and micro system in Japan. It is process technology used to generate micro level integrated system or devices that have combination of mechanical and electrical components. Generalized definition of MEMS can be given as "It is device where micro sensor and mechanical parts (Actuators) along with signal processing circuitry are combined on very tiny piece of silicon." MEMS components generally have micron level dimensioned part, with a moving element which may be solid mechanics type or may fluid one, integrated with some electronic circuit. MEMS is produced using lithography and etching techniques. Besides silicon as substrate other materials like, quartz, glass and polymer are also used as substrate in MEMS devices [1]. Many machines can be built at the same time on the surface of the wafer, without any assembly that is real power of MEMS technology.

MEMS is combination of three basic blocks named as sensor, processor and actuator as shown in Fig. 1.1. Sensor or micro sensor is first block which senses the measurand or input signal. Most of time input is probably non - electrical signal which converts into electrical signal. Non electrical signals may be different possible signals like, thermal, radiation, mechanical, magnetic, optical or bio (chemical). All signals must be converted into electrical signal by sensor using available possible methods of conversion. The basic work with of sensor is shown with vectorial representation in Fig. 1.2(a). Processor is next to sensor block which gets electrical signal from sensor. It does some mathematical or logical operations (decision making operations) on signal. Processor has electrical signal as input and output. The final building block is actuator which has electrical signal from processor as input and generally non - electrical signal as output. It does exactly opposite conversion of signal that is discussed in sensor. It converts electrical signal into non – electrical signals like, thermal, radiation, mechanical,

magnetic, optical or bio (chemical). Actuator's work can be explained with vectorial representation as shown in Fig. 1.2(b). Actuator actually responds to environment (e.g. pumping, filtering, positioning, regulating and moving) based on intended designed instruction [2].

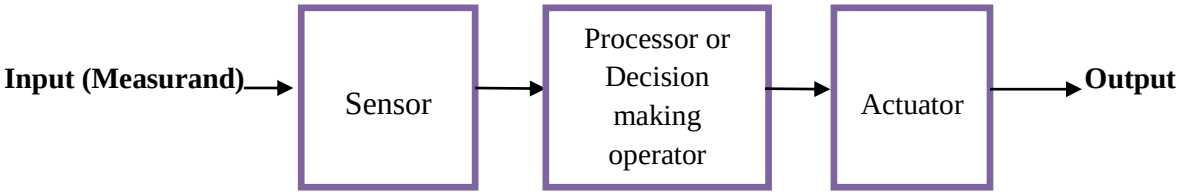

Fig. 1.1 Basic block diagram of MEMS

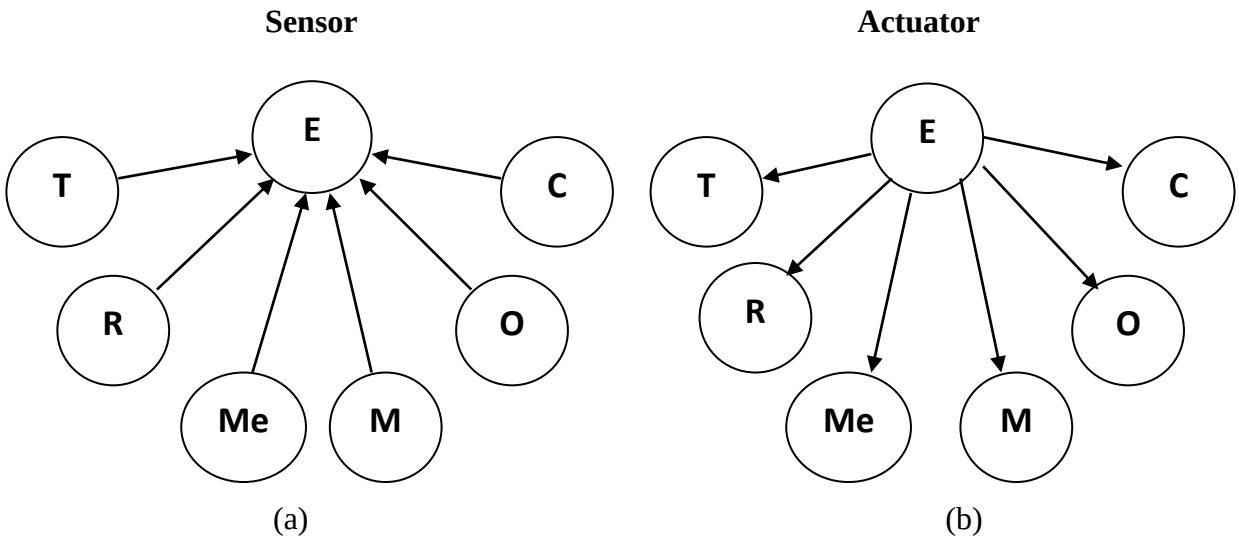

(a) (b)

Fig. 1.2 Vectorial representation of (a) sensor (b) actuator in energy domain space

where E-Electrical, T-Thermal, R-Radiation, Me-Mechanical, M-Magnetic, O-Optical, C - Chemical (Bio)

For fabrication of MEMS, three processing steps are used: (1) Deposition (2) Lithography and (3) Etching. In deposition, thin films of material are deposited on substrate. Two major methods are used for deposition. One is chemical reaction methods which are like, chemical vapor deposition (CVD), Electro deposition, epitaxy and thermal oxidation. Other one is physical reaction methods which are like, physical vapor deposition (PVD) and casting. In lithography, a patterned mask is applied on top of the film by photolithographic imaging. It can be classified in two groups: (1) Pattern transfer and (2) Lithographic module. In etching process, it is necessarily requirement to etch the

films selectively to the mask. Basically, it is subdivided in two methods: dry etching and wet etching.

1.1.2 History of MEMS

MEMS was first developed in the 1970s and then it was commercialized in the 1990s. Using MEMS, it becomes possible to make any system to be smaller, more efficient, less expensive and faster. In an ideal MEMS configuration, ICs (Integrated Circuits) provide the "thinking" part of that system, while MEMS supplement this intelligence with control functions and perception [3]. Pressure sensors having bulk etched silicon structure were the first wave of MEMS commercialization started in the late 1970s and early 1980s. In that first pressure sensor silicon membrane deformed under pressure and piezoresistive track laid on its surface, was affected and the change is used to transform the pressure into an electronic signal [4].

A second wave of commercialization arrived in the 1990s, which was mainly focused on information technology and personal computers (PCs). In this era, video projection is one of the products that was introduced by Texas Instrument which is depended on electrostatic actuated tilting micro mirror arrays. There is another product named thermally operated inkjet print head that remain a high demand application till date.

A micro-optics as an accompaniment to optical fiber communication - by way of all optical related devices and optical switches is the third generation of MEMS commercialization [5]. And the fourth wave of the commercialization could be other applications that may include biological and neural probes, also called lab-on-chip drug development and biochemical system and macroscale drug delivery system. E-nose is also the latest application that comes under fourth generation of MEMS commercialization.

1.1.3 MEMS Materials

MEMS technology may be implemented using different manufacturing techniques and different materials that are totally depend on the device which is being created and the market in which it has to operate [6]. There are different available choices of materials available, as mentioned below:

Silicon

It is the material which is widely used in consumer electronics of the modern industry to create most of the integrated circuits. The cost advantage which gets bigger with increase in output of product, ready availability (abundant), cost effective high quality materials, also capability to incorporate electronic functionality make silicon as attractive choice for a various MEMS applications. It has very suitable material properties among other choices like; it can survive in harsh conditions, has uniform mechanical properties throughout the wafer lots, and also has suitable mechanical, thermal, electrical and optical integration. In a form of single crystal, silicon is considered as almost perfect example of Hookean material, that when it is flexed, there is almost no energy dissipation because it has virtually no hysteresis. Also silicon has very high reliability as this material suffers very little fatigue and also has service lifetime in the range of billions to trillions. And the biggest advantage is fabrication and treatment processes for silicon substrate are documented and well established. Also silicon compounds are also used in MEMS. Some of the examples are Silicon dioxide (SiO_2), Poly-Silicon (Poly-Si), Silicon Carbide (SiC) and Silicon Nitride (Si_3N_4)

Quartz

It is basically a compound of Silicon dioxide (SiO_2) and its orientation is not based on Miller indices. It is also counted as an ideal choice of material for MEMS sensor as it has near absolute thermal dimensional stability. It is advisable material in case of micro fluidics applications in biomedical analysis. It has certain advantages over silicon that it is more dimensionally stable, more flexible in geometry and transparent to ultraviolet light which is better for motive of species detection.

Gallium Arsenide (GaAs)

It is compound semiconductor and is a major candidate for photonics devices as it has high mobility of electrons. It is higher level thermal insulator having outstanding dimensional stability at high temperature. Though it has certain disadvantages compared with silicon like, more difficult to process and more expensive.

Polymers

They are nowadays become popular choice for MEMS and micro system though having biggest drawback of poor conductivity. They have certain proficient advantages like, low cost of raw material, light weight, high electrical resistance, high flexible

structure, high corrosion resistance, and also high dimensional stability. Basically they are divided in two groups: thermoplastics which can be easily formed into desired shape and thermosets which have better temperature resistance up to 350^{o} C and good mechanical strength.

Metals

Metals are generally used to make MEMS elements. Although metals do not have a few advantages which are displayed by silicon materials in terms of mechanical properties, it can exhibit very high degrees of reliability. Metals are deposited by different processes; some of them are electroplating, sputtering and evaporation. Widely used metals in MEMS are: gold, aluminum, platinum, silver, tungsten, copper, nickel, titanium and chromium.

1.1.4 Advantages of MEMS

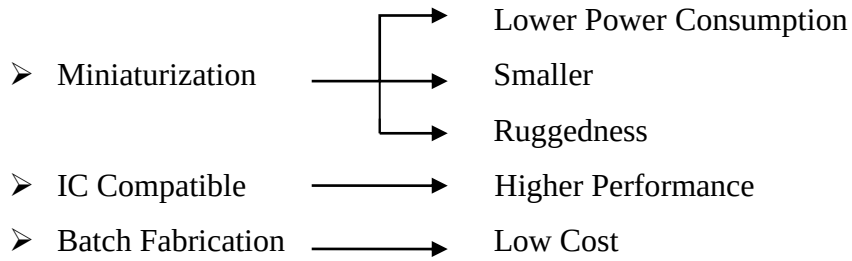

1.1.5 Applications of MEMS

There are so many possible applications for MEMS. Currently, MEMS are most often found as sensors as gas sensors, pressure sensors, optical sensors, position and speed micro sensors but the appliances are making large inroads into defense, medical, aviation, and optical communication [2,3].

Biotechnology

For DNA identification and DNA amplification, MEMS is empowering new discoveries in engineering and science like the Polymerase Chain Reaction (PCR) system. Also there are micro-systems for throughput drug selection and drug screening, micro-machined Scanning Tunneling Microscopes (STMs). For detection of hazardous biological agents and chemical agents, biochips are developed. Bio-MEMS in health and medical related technologies, one important development of Lab-On-Chip for chemo sensor and biosensor is made.

Integrated Circuits

Micro technology generally has been developed with the help of silicon semiconductor. The revolution in silicon has allowed to create reliable, small processor in form of IC (Integrated Circuits). Micro-machined substrates are having significant importance for low power pressure sensors, temperature sensor, gas sensors etc. MEMS based temperature sensors are used for analog and digital temperature detection devices.

Communication

It is more benefiting to make high frequency circuits with the help of RF-MEMS technology. Electrical components like, tunable capacitors and inductors can be enhanced remarkably using MEMS technology. The total circuit area, cost and power consumption can be decreased and the performance of communication circuits can be enhanced if the proper integration of such components are made perfectly. RF-MEMS is widely used in antennas, oscillators, phase shifter circuits and filters.

Automotive Domain

MEMS devices are widely used in airbag system, active suspension, and automatic door locks system. They have large applications in vehicle security systems, headlight leveling systems, and inertial brake lights. MEMS sensors are having application in air temperature control in car.

1.2 Concept of Electronic-Nose (E-nose)

In many industries, for measurement of quality of perfumes, drinks, foods and sometimes chemical and cosmetic products, the human nose is used as diagnostic (analytical) tool [7]. Human sensory panels are highly subjective as human smell estimation is affected by many factors. These individual variations may occur and also be affected by mental health and physical health [8]. One of the great achievement and application of MEMS is E-nose. E-nose is a device which imitates the discrimination of the mammalian olfactory system which is sensory system for smell [9].

The E-nose has sensor arrays which act as olfactory system of human nose that have number of sensing sense [10]. The odour samples sense on the array sensing surface causes a chemical and/or physical change on that surface which changes associated electrical properties of sensing surface like, conductivity or current.

1.2.1 E-nose sensor response to odorants

E-nose sensors' response to odorants is normally observed as a 1st order time response. In the very first stage of odour testing, it is necessary to acquire a baseline by flushing a reference gas by sensor. When it is exposed to that odorant, it causes variations in output signal till the sensor attains to steady-state value. Finally the odorant is removed from the sensor by using the help of reference gas and it comes back to its original baseline value. Here this process gives two important definitions.

Response time: It is the time taken by for the sensor to sense (expose) the odorant.

Recovery time: It is the time taken by sensor to come back to its baseline resistance value.

The succeeding stage in this odour analysis is sensor response manipulation that is obviously with respect to baseline value and this process reduces drift, noise and also naturally generated large or small signals [8].

Some common sensors used for E-nose are:

- **Intrinsically conducting polymers sensor:** When vapor / gas is flushed on surface of conducting polymers, conducting polymers expand and its resistance will be changed that cause change in conductivity.
- **Composite Conducting polymers sensor:** They have combinations of conducting polymer and non-conducting particles. Typically conducting polymers like, carbon black and polypyrrole (PPy) scattered in an insulating polymer matrix (non - conducting).
- **Surface acoustic wave (SAW) sensor:** In surface acoustic wave sensor, input transducer, gas sensitive coating and output transducer is deposited on piezoelectric substrate. As input transducer gets ac input, it generate acoustic wave. There is change in mass of gas sensing membrane that causes alteration of acoustic frequency produced by input transducer. This change is observed by output transducer.
- **Quartz crystal microbalance sensor:** It works on same principle as SAW sensor. Normally, piezoelectric material oscillates while ac supply voltage is applied and it produces resonance frequency. But gas is absorbed by this material and it changes its mass and that makes change in resonance frequency.
- **Optical sensors:** Glass fibre coated with dye saturated polymer is used for sensing purpose. At one end of fibre, light is entered with original wavelength and

due to gas interaction of fibre at the other end, there is shift in wavelength is observed.

- **Metal oxide field effect transistor (MOSFET) sensors:** The basic concept of metal oxide field effect transistor (MOSFET) sensor is that there is variation in oxide conduction while it interacts with a gas. Also this variation is normally proportional to the amount of gas concentration.

1.2.2 Applications of E-nose sensor

E-nose has countless applications in many areas such as food products, agriculture field, medical field, military etc. All these applications are explained as below.

1. **Agriculture Field:** E-nose is used in crop protection, plant production, to find plant harvest timing, to find crop (fruit) ripeness, to find pre & post harvest diseases, pest identification [11].

2. **Pharmaceutical and Medical:** Its applications are in product purity checking, quality control of drugs, consistency and uniformity of drug formulation, cancer detection, Urinary Tract Infections (UTI) detection, respiratory diseases recognition and other clinical discovery [12,13].

3. **Manufacturing:** E-nose is widely applicable in hazardous gas leak detection, to inspect flavor and aroma, safety & security, examine manufacturing process [11].

4. **Food & beverage:** It is utilized in product variety analysis, product evenness checking, smell reorganization, quality assessment, smell characteristics checking, milk (dairy) product checking, meat and sea food quality checking etc [11,14].

5. **Military:** Explosive substance detection, military and civilian safety and security, also chemical and biological weapons detection etc are applications of E-nose in military [15].

6. **Environment:** It is used in hazardous gas identification, pollution detection, water & air quality checking etc. [16,17]

7. **Aroma and Cosmetics:** Its application may be in **c**omparison natural and artificial cosmetic products, to major efficiency of deodorants, to find life time of perfume etc. [15].

There are wide range of application in scientific research area and chemistry (chemical fluid/ gas detection).

1.3 Metal Oxide Gas Sensor

Although we have already discussed all options for gas sensor used in E-nose in topic 1.2.1, metal oxide sensor is the best option as it has certain advantages as mentioned below [16].

- Easy electronic interface
- Capability to detect no. of gases
- Ease of use
- Very low maintenance
- Good sensitivity
- Low cost
- Fast response time and recovery time.

There are two available options of MOSFET sensors. One is n-type sensors (sensing surface) which have majority charge carriers as electrons such as ZnO (Zinc Oxide), TiO_2 (Titanium dioxide), WO_3 (Tungsten trioxide), Fe_2O_3 (Iron (III) oxide) etc. While another is p-type sensors (sensing surface) having holes as majority charge carriers such as NiO_2 (nickel oxide), CoO (cobalt oxide) and others. MOSFET sensors surface is highly sensitive with oxidizing gases (such as N_2O, CO_2, NO_2, and NO etc.) which cause increase in depletion region of sensing surface and reducing gases (such as NH_3, CH_4, SO_2, H_2S and CO etc.) which cause decrease in depletion region of sensing surface [16]. This slight change of depletion region causes electrical properties of material from that amount (concentration) of certain gas can be measured.

1.4 Need of micro-heater

In metal oxide sensor which uses electron depleted surface, either oxidation or reduction process occur on depleted sensing surface or oxide surface. In these process electrons are added or extracted depending on metal oxide sensor whether is n-type or

p-type. But all these process generates oxygen species like, O^-, O_2^- and O^{-2} [16,18]. It needs very high temperature (around 100^o C to 600^o C) to occur this phenomena depending upon the gases and used sensing surfaces.

To achieve this high temperature in metal oxide sensor, there is a need of micro-heater (sometimes it called as heating element or heater). The main task of micro-heater is to provide temperature uniformity (with attaining constant high temperature) for sensing layer. Also micro-heater must operate at less applied voltage so power consumption can be reduced. If micro-heater is in direct contact with substrate, it may damage substrate. So generally, micro-heater is placed on platform of SiO_2 (Silicon dioxide).

1.5 Structure of metal oxide based gas sensor

In any metal oxide based gas sensor structure has basically five layers (as shown in Fig. 1.3):

- Substrate
- Insulating platform
- Micro-heater
- Interdigitated electrodes
- Sensing Film

Substrate:

Silicon is considered as the best choice as substrate in all the integrated circuits, all the electronic consumer products and MEMS as well. Its advantages are already discussed in above section.

Insulating platform:

To give electrical insulation, a thin layer of SiO_2 (Silicon dioxide) or sometime Si_3N_4 (Silicon Nitride) is used. This is helpful to avoid direct damage on substrate due to micro-heater as micro-heater is heated up to 100^o C to 600^o C.

Micro-heater:

MEMS based metal oxide structure is very small in terms of surface (around some hundreds of μm^2 surface area). There is a need of micro-heater to proper detection of desired gases. As micro-heater geometry in the range of micron dimension, it requires very low applied voltage to achieve very high temperature. The heating of micro-heater is

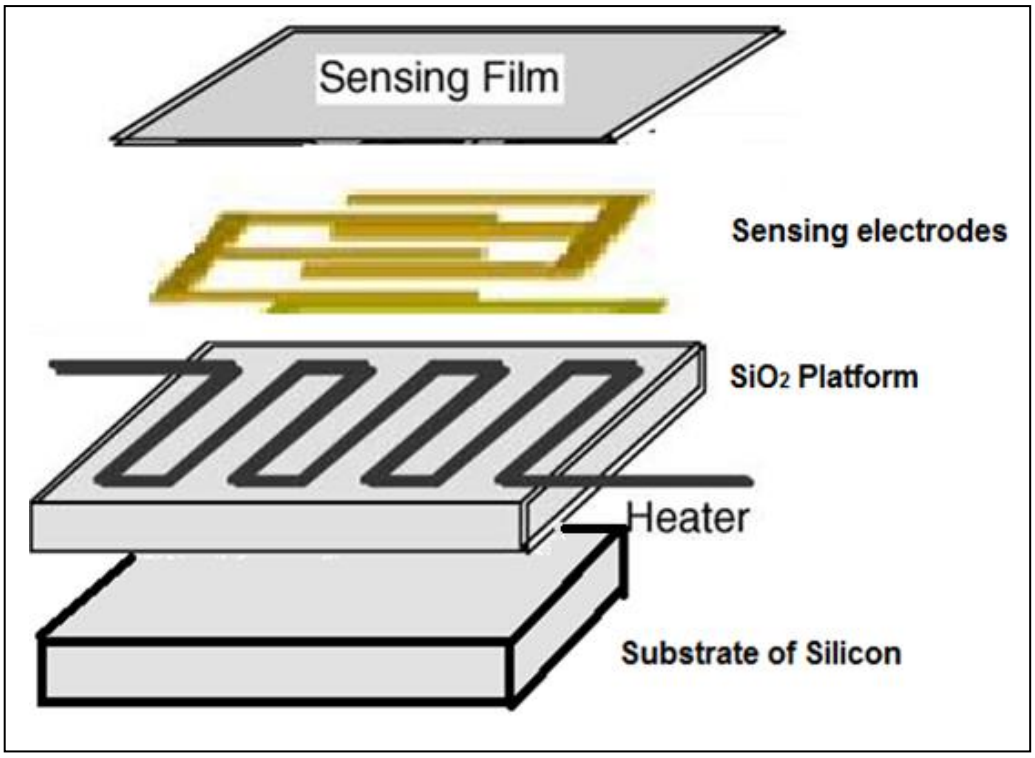

Fig. 1.3 Basic structure of metal oxide based gas sensor

based on joule heating concept. Micro-heaters are extensively used in humidity sensors, microfuidics, gas sensors and many other micro systems. Micro-heater is very crucial component of metal oxide gas sensors.

Interdigitated electrodes:

On the SiO_2 platform, micro-heater is placed and there is interdigitated electrode made of aluminum or gold is placed which detect variations in resistance of metal oxide sensing surface while it responds to gases.

Metal oxide sensing layer:

There are several options available for metal oxide sensing layer. The concentration of any gases on the sensing surface is measured in terms of ppm (part per million) or ppb (part per billion). The resistivity / conductivity of sensing surface changes with amount of gas concentration. The temperature limit of some selected metal oxide sensing surface are shown in Table 1.1 [19].

Table 1.1 Temperature limit of some selected metal oxide sensing surfaces used in gas sensors [19]

Sr. No.	Metal Oxides sensing surface	Temperature limit/ range
1	Tin oxide (SnO_2)	300° C or above
2	Zinc oxide (ZnO)	300° C
3	Tungsten trioxide (WO_3)	Up to 500° C
4	Indium tin oxide (ITO)	300° C
5	Titanium oxide (TiO_2)	250° C
6	Cerium oxide (CeO_2)	400° C

As metal oxides have very good sensitivity to some hazardous gases, there are utilized for sensing purpose. Some typical metal oxide sensing surface and aimed gases are shown in table 1.2 [16,20].

Table 1.2 Typically used metal oxide sensing surface and their aimed gases [16,20]

Sr. No.	Metal Oxides sensing surfaces	Aimed gas
1	Tungsten trioxide (WO_3), Zinc oxide (ZnO)	Nitrogen dioxide (NO_2)
2	Tungsten trioxide (WO_3)	Nitric oxide (NO)
3	Tin oxide (SnO_2), Zinc oxide (ZnO)	Nitrous oxide (N_2O)
4	Tungsten trioxide (WO_3), Zinc oxide (ZnO)	Hydrogen sulfide (H_2S)
5	Zinc oxide (ZnO), Titanium oxide (TiO_2)	Carbon monoxide (CO)
6	Titanium oxide (TiO_2), Tin oxide (SnO_2)	Ammonia (NH_3)
7	Tungsten trioxide (WO_3), Tin oxide (SnO_2), Zinc oxide (ZnO)	Methane (CH_4)
8	Tungsten trioxide (WO_3), Zinc oxide (ZnO), Tin oxide (SnO_2)	Sulfur dioxide (SO_2)
9	Zinc oxide (ZnO), Tin oxide (SnO_2)	Carbon dioxide (CO_2)

1.6 Literature Review

Testuro Seiyam et al. in 1962 designed a new detector for sensing gaseous components using borosilicate glass tube and zinc oxide (ZnO) as sensing film. The resistance change is observed by electronic recorder without amplification. Results are analyzed for Toluene, Benzene, Ethyl ether, Propane, Carbon dioxide. Electronic recorder output time response is observed and results show peaks in output which represents change in thermal conductivity of ZnO [21].

H. Meixner et al. in 1996 have reviewed some usual metal oxides like, ZnO, SnO_2, and TiO_2. They have also explained that other metal oxides are less examined due to lack of knowledge at that time. They have discussed basic requirements of metal oxides in next generation. They should have low cross sensitivity, high reducibility, long term stability and less breaking time [22].

Martin Hausner et al. in 1997 have designed gas sensor having Tin oxide (SnO_2) as sensing layer and have used buried poly-Si (poly Silicon) micro-heater on silicon substrate with sandwich thermal oxide layer. Two pairs of interdigitated electrodes are used and they have observed that long term drift (from the baseline) is significantly reduce and by providing addition gate potential selectivity can also be enhanced [23].

Marius Dumitrescu et al. in 1998 have simulated poly-Si based hotplate structure for surface area 110 µm x 110 µm with silicon as substrate. 3D finite element method in "COSMOS" program is used for simulation of two structures named with four "poly" suspended bridges and a pillar supporting at central with separation of 1 µm air gap to substrate. They have achieved high temperature of 673 K (400^o C) by applying 100mW power [24].

S. Semancik et al. in 2001 have introduced microhotplate platform made of poly-Si on the platform of SiO_2. They have used four arrow shaped electrodes for measuring heating temperature and observing change in sensing surface. Microhotplate is CMOS compatible and easily integrated on heterogeneous types of on chip circuits [25].

Isolde Simon et al. in 2001 have reviewed both closed membrane type metal oxide gas sensor and suspended membrane type gas sensor. They have discussed sensing layer deposition techniques like, thick film deposition method and thin film deposition method.

Also they come with conclusion that both sensing film differ from their thickness and micro structure and that leads to different transducer functions [26].

M. Afridi et al. in 2002 have explained monolithic MEMS based gas sensor with poly-Si micro-heater. Gas sensor virtual components that are analog circuits and sensor itself should enclose in digital cell so one can make digital interface. They have concluded that system response time is depended on sensor and its complexity. Heater efficiency, temperature sensor response and sensing film response with respect to gas concentration are analyzed [27].

M. Baroncini et al. in 2004 have proposed double spiral micro-heater configuration with four point probes for MEMS gas sensor. They have used silicon as substrate and Si_xN_y as membrane of 1 mm^2 surface area. They have implemented double spiral geometry with two probes for voltage tab (VT) and two probes for micro-heater ends. Also sensing layer has two probes for measuring change in electrical properties. Surface temperature vs heating power characteristic is analyzed [28].

J. Cerd`a Belmonte et al. in 2006 have described implementation and fabrication process. They have made structure of Si_3N_4 layer on both side of silicon substrate. Also have SiO_2 insulating layer above Si_3N_4 layer and it has Ti/Pt micro-heater suspended on the top of the structure. They have used $BaSnO_3$ as sensing surface. Results are analyzed (resistance variation) at 600^o C and 700^o C for O_2 and CO gases [29].

Ching-Liang Dai et al. in 2007 have implemented on chip nanowire WO_3 (sensing material) based humidity sensor with a poly-Si micro-heater and an inverting amplifier using CMOS process. Due to micro-heater sensing film is heated and overall surface resistance is connected as feedback resistance of inverting amplifier. Humidity vs output voltage characteristic is observed [30].

J.F. Creemer et al. in 2007 have introduced TiN (Titanium nitride) as material for micro-heater and microhotplate. They have compared spiral geometry structure for platinum and TiN micro-heater. Results are compared and analyzed and they have investigated that TiN have high melting point so it can survive very high temperature than platinum micro-heater [31].

H.-Y. Lee et al. in 2008 have come out with Wheatstone bridge (circular ring) platinum based micro-heater structure that work as four resistance is equal in normal condition and change can be measured with analog circuitry. This structure has multi-ringed that help to spread heat so more uniformity can be achieved. They have used SiO_2 – Si_3N_4 – SiO_2 (O/N/O) structure with platinum as micro-heater. Also they have proved that using this structure high uniform temperature of 400^o C is achieved at central area of circular ring micro-heater [32].

Velmathi G. et al. in 2010 has introduced six different geometries of micro-heater. They have used finite element method in COMSOL Multiphysics simulation tool. They have analyzed plane plate with central square hole, double spiral, honey comb, meander, fan type and s-type of geometries. Their 2D surface temperature is observed to achieve 400^o C temperature. Also resistive heating vs applied voltage characteristic is analyzed [33].

Jae-Cheol Shim et al. in 2010 have fabricated Nitric oxide sensor using 3C-SiC (cubic unit cell, zinc blende) material based micro-heater with Zinc oxide (ZnO) sensing film. They have used AlN/SiC as membrane. They have analyzed that platinum added ZnO have high sensitivity as compare with only ZnO sensing film. Also they have proved that SiC micro-heater can withstand till power value of 1.1 W that is quite higher than platinum micro-heater [34].

M. Gayake et al. in 2011 have compared three different geometries of Polyimide based micro-heater using finite element method of COMSOL Multiphysics simulation tool. They have changed track width and gap width of all three geometries and come out with conclusion that circular geometry has better response due to less edge losses. Also for micro-heater, heating response is observed using 5.2 V and 6.0 V supply voltage and noticed that 6.0 V supply giving good heating response [35].

Vineet Bansal et al. in 2011 have simulated platinum spiral geometry using finite element method of COMSOL Multiphysics simulation tool. They have investigated for different cases (1) simple spiral micro-heater that gives temperature up to 761.73 K (2) Spiral geometry with Si cavity at central that has temperature response up to 1036.8 K (3) a suspended spiral micro-heater on four bridges that provides maximum temperature up to 919.1 K and (4) spiral micro-heater with sensing layer of ZnO on top (complete gas

sensor) which gives 670.31 K temperature. Also effect of micro-heater thickness is simulated and relation with temperature and power consumption is plotted [36].

Susmita Sinha et al. in 2011 have simulated various shape of micro-heater named, meander shape, curved meander shape, double spiral meander shape, curved double spiral meander shape, s-shape and fan shape. They have used finite element method of COMSOL Multiphysics 4.0. They have used DilverP1 (which is made of alloy of Ni, Co, Fe) material for micro-heater. Transient temperature response and relation between maximum temperature and power consumption is analyzed also have proved that power consumption of DilverP1 is less compare with poly-Si and platinum [37].

Bijoy Kantha et al. have made 3D analysis of MEMS based Dilver P1 based micro-heater with Coventorware design and simulator software. Structure has insulating layer as Si_3N_4, interdigitated electrodes of Au and sensing material as ZnO. Thickness and power consumption relation is observed and voltage and power consumption relation for different thickness of micro-heater is analyzed [38].

L. Sujatha et al. in 2012 have done simulations for poly-Si based micro-heater using finite element method of COMSOL Multiphysics 4.2 simulation tool. Four different geometries named, single meander, double meander, fan type and square type are simulated and 2-D simulation response is analyzed. Maximum temperature value and temperature uniformity are analyzed and they have concluded that square type geometry has better temperature uniformity among all. Maximum temperature and applied voltage relation is plotted [39].

Jianhai Sun et al. in 2013 have made flow sensor having silicon as substrate and SiN as insulating layer. They have used two heating/sensing elements to sense resistive variation which they are diagonal so works as Wheatstone bridge connection. Variation in resistance can be observed as amplifier output voltage [40].

Monika et al. have simulated curved spiral micro-heater geometry using Dilver P1 as micro-heater material using finite element method analysis of COMSOL Multiphysics. Micro-heater thickness is varied and power consumption is analyzed. Also simple curved micro-heater and with silicon membrane curved micro-heater are simulated. Power consumption of same curved spiral micro-heater which made of different material are

investigated and have proved that Dilver P1 based micro-heater gives result with minimum power consumption.

1.7 Objectives

The main objectives of presented work are as follows:

1. To describe and simulate different micro-heater geometries using COMSOL Multiphysics 4.3 and to analyze which geometry gives better temperature uniformity.
2. To achieve a geometry optimization in fixed surface area for given structure for temperature uniformity.
3. To optimize semiconductor material or metal for micro-heater which consume less power and give better temperature uniformity.
4. To analyze steady state response of different parameters of micro-heater.

1.8 Thesis Organization

Chapter 2 covers the research methodology used in this project. Finite element analysis (FEA) package of COMSOL Multiphysics 4.3 is used for design and simulation of micro-heater geometries of metal oxide based gas sensor. Different modules and physics are describe also study types are explained. Joule heating and thermal expansion physics of Structural mechanics module is used to generate micro-heater geometries. Computer simulation has certain advantages because it provides design optimization by changing materials of the device, its properties, geometries and layer dimensions without actual fabrication .This approach can be helpful to minimize cost and time of real fabrication.

Chapter 3 describes the design parameters of metal oxide gas sensor. It explain the design parameters of micro-heater and effect of this parameter on sensing surface of MEMS based metal oxide gas sensors.

Chapter 4 explains different micro-heater geometries comparison for gas sensor and best shape is selected among all the choice for improving temperature uniformity in gas sensor for proper detection of hazardous gases.

Chapter 5 gives shape optimization of selected micro-heater geometry to enhance better temperature uniformity. It gives relation between maximum surface temperature with

applied voltage, also relation between maximum surface temperature with thickness variation. All steady state analysis is done and parameters are compared for poly-Si and platinum based micro-heater.

Chapter 6 describes the fabrication steps to design micro-heater for MEMS based gas sensor. This will helpful to fabricate MEMS based gas sensor with Poly-Si and/Platinum based micro-heater.

Chapter 7 concludes this project after all results compared in Chapter 5. Also it gives idea about future work possible in this field.

2.1 COMSOL Multiphysics: An Introduction

It is powerful tool which provides Finite Element Analysis (FEA), solver, simulation. It has packages (modules) for engineering and general physics applications which are based on advanced numerical method so it is generally called as "Multiphysics". In early year, this software is known as "FEMLAB". The basic idea of this tool is to mimic as similarly as possible effects that are noticed in real world. This tool also offers to add coupled system of PDE (Partial Differential Equations). It provides simulation platform along with their dedicated physics tools for AC/DC module, electrical, chemical, plasma, general physics etc.

With the help of built in interfaces and modern support for defining material properties, it is very easy to make models implementing the suitable physical quantities such as, constraint, supply sources, fluxes (electrical or heat) , its material properties without specifying the underlying equations [41]. This tool has number of equations that representing any model which has been chosen for analysis. User can define own expressions, variables and terminals. COMSOL basic window is shown in Fig. 2.1.

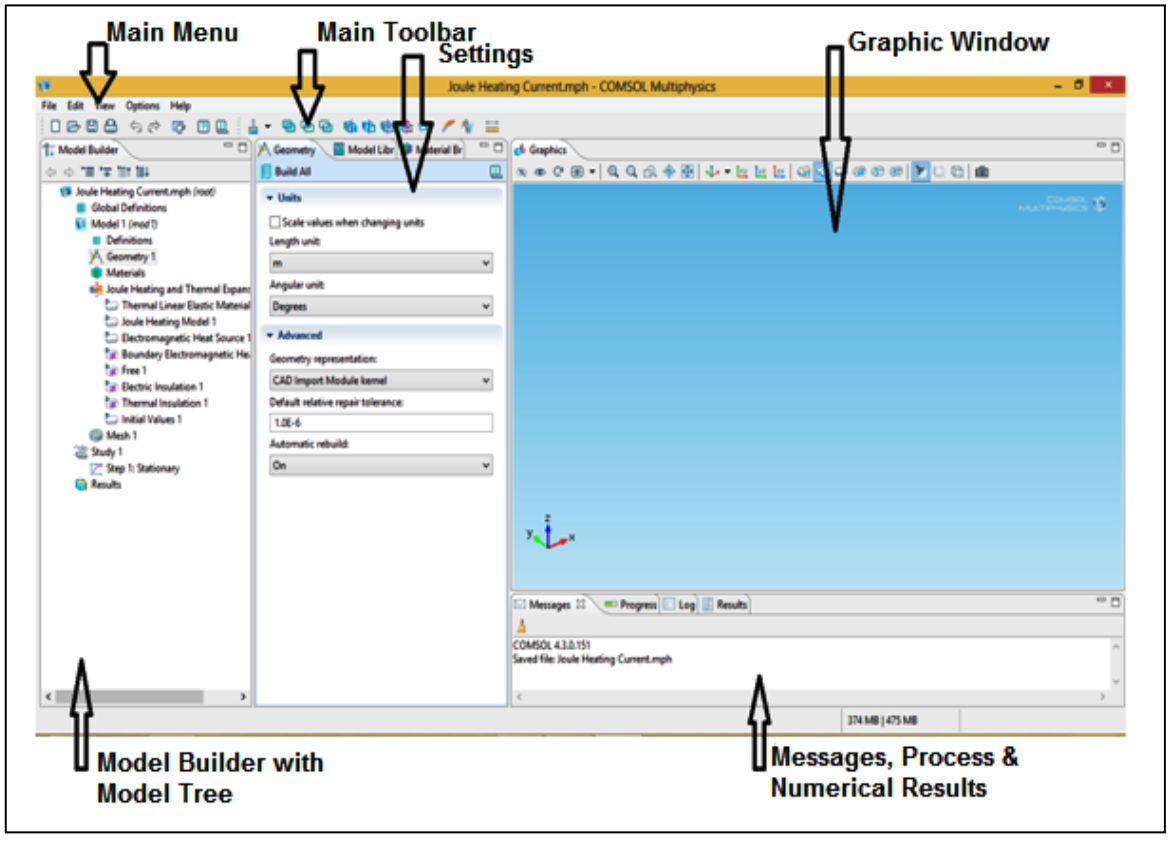

Fig. 2.1 COMSOL Multiphysics window

First, user has to add his/her physics with specific sub-physics (Specific area of simulation or specific operation of that physics). Also user has to define study type for analysis. Study types options are mentioned below:

- Preset Studies
  - Eigen Frequency
  - Stationary
  - Time Dependent
- Custom Studies
  - Empty Study
  - Eigen Value
  - Frequency Domain

One can change/add study during simulation process also. There are many available choices like, parametric sweep response, cluster computing etc. Fig 2.2 shows setup study tab on simulation window.

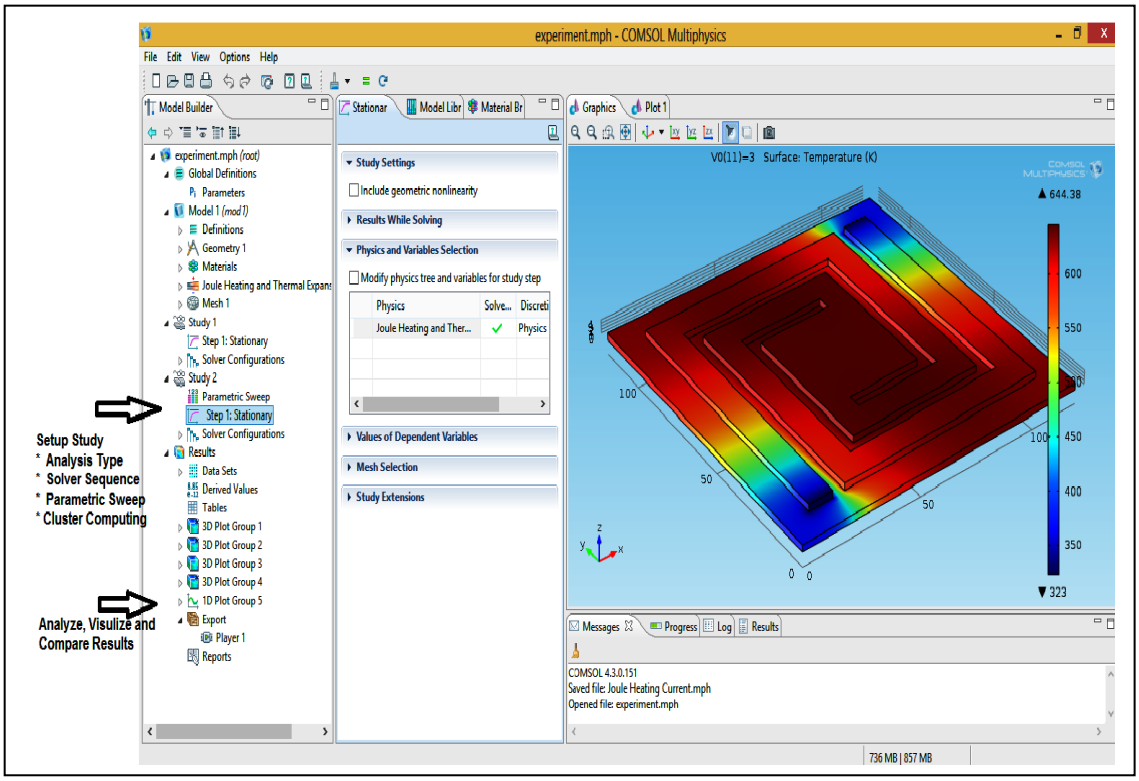

Fig. 2.2 Setup study type in COMSOL Multiphysics

COMSOL Multiphysics supports many applications area. It also provides some live link module such as with MATLAB, CAD and Excel.

All the application modules are mentioned in the list:

- AC/DC Module
- Acoustics Module
- Batteries & Fuel Cells Module
- CAD Import Module
- CFD Module
- Chemical Reaction Engineering Module
- Corrosion Module
- ECAD Import Module
- Electrochemistry Module
- Electrodeposition Module
- Fatigue Module
- Geomechanics Module
- Heat Transfer Module
- LiveLink Products for CAD
- LiveLink for MATLAB
- LiveLink for Excel
- Material Library
- MEMS Module
- Mixer Module
- Microfluidics Module
- Molecular Flow Module
- Multibody Dynamics Module
- Nonlinear Structural Materials Module
- Optimization Module
- Particle Tracing Module
- Pipe Flow Module
- Plasma Module
- RF Module
- Semiconductor Module
- Structural Mechanics Module
- Subsurface Flow Module
- Wave Optics Module

2.2 Joule Heating and Thermal Expansion Interface

The Joule heating and thermal expansion interface (Physics) is found under the **Structural Mechanics** branch in the **model wizard window.** It has combination of Heat transfer interface, electric current interface and also Structural Mechanics interface.

The Joule Heating Interface

The Joule Heating physics is combination of two different modules: electric current interface which is part of AC/DC module and Heat transfer interface. Joule heating is also called as resistive heating or ohmic heating.

As mentioned earlier, there is interaction of both modules, which may occur in both directions:

1. In the Electromagnetic Heat Source node, this resistive heating is visible as a heat source.
2. To use default setting value for electric conductivity from the material. From the choice from Conduction current→ Electrical Conductivity list, and choose the Linearized resistivity which is basically temperature dependent and describe by following equation.

$$\rho = \frac{\rho_0}{\left(1+\alpha\left(T-T_0\right)\right)} \qquad (2.1)$$

Where α is the temperature coefficient of resistivity, which describes how the resistivity varies with temperature and ρ_0 is the resistivity at reference temperature T_0.

We can do analysis in 2D, axis symmetric 2D and 3D. The dependent variables may be temperature T and electric voltage potential V. Joule Heating and Thermal Expansion physics is selected and parameters are defined for the structure under analysis which is shown in Fig. 2.3. They are interface parameters; we can add more parameter as per our requirements of parameter definition by simply right clicking on Joule Heating and Thermal Expansion physics. Generally we add parameter definition like, Fixed constraint from Structural Mechanics, Ground and Electric Potential from Electric Current, Temperature and Heat Flux from Heat Transfer physics defined under main module.

They are defined like [42],

- Thermal Linear Elastic Material
- Joule Heating Model
- Electromagnetic Heat Source
- Boundary Electromagnetic Heat Source
- Free
- Electric Insulation
- Thermal Insulation
- Initial values
- Terminal
- Ground
- Heat Flux
- Temperature
- Fixed Constraint

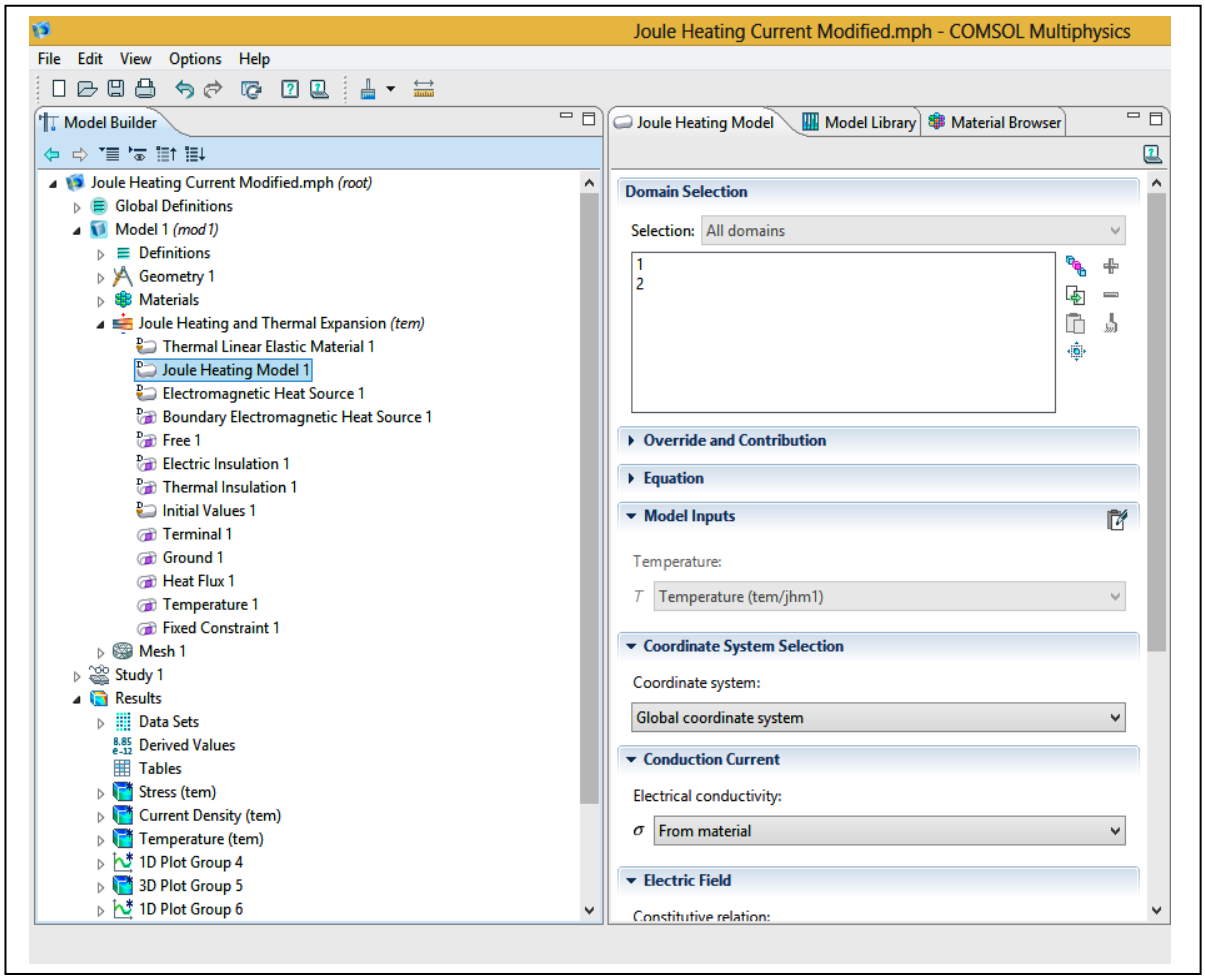

Fig. 2.3 Joule Heating and Thermal Expansion module window in COMSOL Multiphysics

2.3 Electro – Thermal Mathematical Modeling in Joule Heating

Joule Heating model contains the following important sections:

Domains

While analyzing any structure, one should select the domain on which he/she wants to apply Joule Heating and Thermal Expansion model, otherwise it select all domain by default [43].

Dependent Variables

The Joule Heating Model node in COMSOL uses the following version of the heat equation as the mathematical model for heat transfer in solids:

$$\rho C_p \frac{\partial T}{\partial t} - \Delta(k\Delta T) = Q \tag{2.2}$$

With the following material properties:

- $\boldsymbol{\rho}$ is the **density**.
- $\boldsymbol{C_p}$ is the **heat capacity.**
- $\boldsymbol{k}$ is the **thermal conductivity** (a scalar or a tensor if the thermal conductivity is anisotropic).
- **Q** is the **heat source** (or sink).

For Joule heating, it comes from the electric current and is added in the Electromagnetic Heat Source node. For a steady-state condition, obviously temperature does not vary with time so we can eliminate first term. In addition, an electric current equation is also added in analysis.

When an electric current flows in a solid or in liquid having finite conductivity, it converts electric energy into heat through material resistive losses which is widely known as joule heating. Resistive heat generated Q is proportional to square of current density J . Electric field E is equal to negative of gradient of voltage potential V. Also there is proportional relation between current density J and electric field E and there is reciprocal relation between conductivity σ which is function of temperature and a resistivity ρ. From the above discussion,

$$Q \propto |J|^2 \tag{2.3}$$

$$\sigma = \sigma(T) \tag{2.4}$$

$$\rho = \frac{1}{\sigma} \tag{2.5}$$

$$Q = \rho \cdot |J|^2 = \frac{1}{\sigma}|\sigma \cdot E|^2 = \sigma \cdot |\nabla V|^2 \tag{2.6}$$

For particular temperature range, the electric conductivity σ is a function of temperature T according to:

$$\sigma = \frac{\sigma_0}{1 + \alpha(T - T_0)} \tag{2.7}$$

Where α is the temperature coefficient of resistivity, which describes how the resistivity varies with temperature and σ_0 is the conductivity at the reference temperature T_0. Also power consumption is describe as,

$$P = \frac{V^2}{R} \tag{2.8}$$

Where V is electric potential applied and R is resistance of heating electrode. As explained in (7), power consumption is directly proportional with square of applied voltage and also inversely proportional with the resistance of used material.

The equations have been solved and simulation is done under Dirichlet, Neumann, and mixed boundary conditions using the Finite Element Analysis (FEA) method when the Electro-Thermal module is selected in COMSOL Multiphysics 4.3. Also for simulation purpose, fixed applied electrical potential and fixed temperature and the ends of the material terminal is considered.

2.4 Model Inputs

This section contains values and fields, which are considered as inputs to expressions that define material property. If you have added such user defined property groups, their model inputs appears here. Initially, it is empty section.

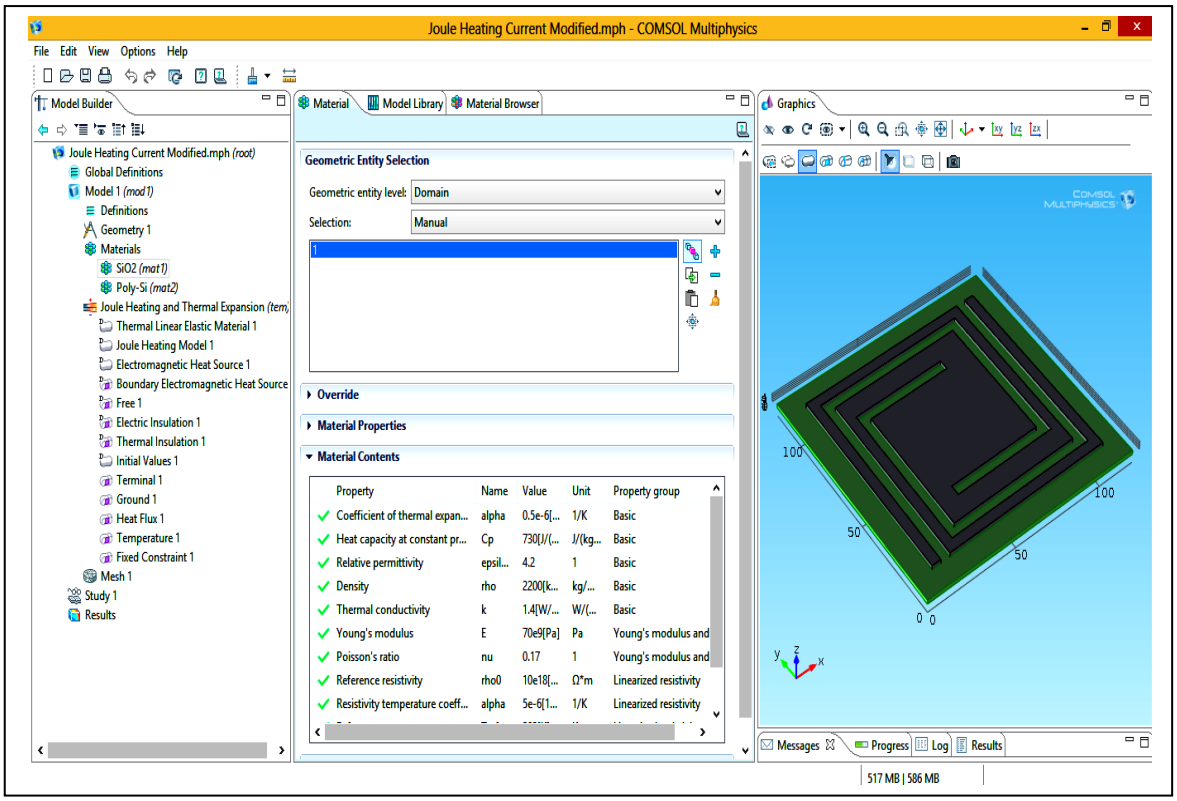

Fig. 2.4 Material Selection in COMSOL Multiphysics 4.3

Conduction Current

It has SI unit of S/m and it defines electrical conductivity. WE have already discussed this in previous section. Used have to go to Joule Heating and Thermal Expansion Model→ Joule Heating Model → locate Conduction Current → Electrical Conductivity and have to change it from user defined to Linearized resistivity.

Heat Conduction

There is default setting to use the thermal conductivity from the material. If anyone wants to give his/her own value, select option of user defined. It has SI unit as [W/(m.K)]. The thermal conductivity k gives relation between the temperature gradient ΔT and the heat flux vector q. Path will be Joule Heating and Thermal Expansion Model → Joule Heating Model → locate Heat Conduction → choose option as from material.

Electromagnetic Heat Source

The Electromagnetic Heat Source feature is only available in the Joule Heating predefined COMSOL Multiphysics interface. It is added as default node. Joule heating is proportional to I^2R, where I is electric current and R is resistance of material.

Initial Values

The initial Values node adds initial values for the temperature T and the electric potential V that can serve as an initial condition for a transient simulation or as an initial guess for a non linear solver. If users need to specify more than one set of initial values, then one can add addition Initial Values features. Generally, temperature is taken as room temperature (293.15 K) and electric voltage potential is 0V.

Free

Free feature is considered as default boundary condition. That means that there is no loads and/or no constraint acting on boundary. In micro-heater, this feature is used for edge.

Ground

This feature is not given directly but we have to choose by right click on Joule Heating and Thermal Expansion Model and choose electric currents then choose ground option. In micro-heater, we have to define one end as electric potential and other as ground.

Fixed Constraint

We have to make fix structure sometimes domain or edges or boundary to withstand against stress and joule heating. It may change structure. So there is one option available by right clicking Joule Heating and Thermal Expansion Model →Structural Mechanics → Fixed Constraint.

2.5 Conclusion

In this chapter, we have studied and discussed about the COMSOL Multiphysics 4.3 simulation tool with its features and different modules. As we will design and simulate different micro-heater geometries, this module will helpful to analyzing results and understand the behavior of micro-heater with respect to its properties.

CHAPTER-3

3.1 Sensor design parameters

As already discussed earlier, there is a need of micro-heater for proper detection of desired gases in any metal oxide gas sensor. Sensing surface heating can be raised by micro-heater using Joule heating effect, varying thickness of micro-heater geometry or choosing preferably dielectric for material. In this work, various micro-heater geometries are analyzed to find optimum solution of micro-heater. Gas sensor made with this optimized micro-heater should have some basic parameters like, low power consumption, high sensitivity, low response/recovery time, stability and good lifetime.

Power Consumption

Power consumption is very crucial parameter for any electronic device. It should have minimum for any device to work that device at low power. For micro-heater, power consumption can be reduced by decreasing device area and confining heat in particular geometry. It is necessary to have micro-heater with thermal insulation with rest of geometry for better heater confinement. The thermal losses in micro-heater are coming from three sources: heat radiation, transfer of heat from one place to another place (Convention loss) and conduction from membrane.

Convention loss is dependent on the micro-heater area (it can be reduced) and radiation loss is not that much (negligible) at 400^{o} C. Micro-heater material should have low thermal conductivity to reduce heat loss. Parameters like, resistive heating area, total device area and membrane area should reduce to decrease overall thermal loss.

Lifetime

While voltage potential is applied to micro-heater, there is a thermal stress induced in the gas sensor (specifically in micro-heater). The stress is generated due to mismatch in the thermal expansion coefficient in different materials used in gas sensor. Also when we are achieving high temperature in micro-heater, there is change of crack in geometry or in sensing film so sensor should have high mechanical stability for better lifetime.

Response time

This response time can be defined as time required to reaching 67% of the saturation value. This time is basically corresponding to the response of sensing film. It is

necessary to have fast response time (minimum value) where the sensor is placed in dynamic atmosphere. This time can be decreased by reducing the thinness of membrane as it reduces thermal mass.

Stability

It is the capability of a gas sensor to provide reproducible results for certain time duration. This includes retaining to output parameter such as, sensitivity, selectivity and recovery/response time.

Sensitivity

This is defined as minimum amount of input required to produce specified output. The sensitivity 'S' is expressed below [44,45]:

$$S = \frac{R_a - R_g}{R_a} = \frac{\Delta R}{R_a} \tag{3.1}$$

Where R_a is sensor resistance in air, R_g is resistance in test gas and ΔR is change in the resistance in presence of reducing gases.

Selectivity

The sensor output may change when it is affected by other environment variables or parameters. This may appear as noise or unwanted signal. Also the sensor is said to be non-sensitive. It traditionally defines specificity or selectivity by taking system of n sensors, each with output value y_k (k= 1, 2…n). The value of partial sensitivity can be explained as the measured value of output of sensitivity at k^{th} sensor to interfering quantities or variables X_j as,

$$S_{jk} = \frac{\Delta y_k}{\Delta X_j} \tag{3.2}$$

3.2 Micro-heater

MEMS Micro-heaters has ability to generate very high temperature at low power consumption. They also exhibit fast response time. Generally micro-heaters are having a thin film heater coil or wire which may suspended within silicon for better thermal isolation. Usually, micro-heaters have platform of Silicon dioxide (SiO_2) or Silicon nitride (SiN). The overall surface temperature can be found by measuring the change in electrical resistance of micro-heater or they have separate electrodes available to measure this temperature as shown in Fig.1.3. They are capable to operate at temperature up to 600^o C.

The power consumption or heating power (P) can be calculated using formula as explained below:

$$P = \frac{V^2}{R} \tag{3.3}$$

Where V is an applied voltage and R is a resistance across two ends of micro-heater.

The value of resistance can be found by mentioned formula for given micro-heater geometry:

$$R = \rho \frac{l}{w \cdot h} \tag{3.4}$$

Where ρ the value of resistivity of material, l is the length, w is the width and h is the height of micro-heater.

A structure of micro-heater is shown in Fig. 3.1, where 120 x 120 μm^2 platform of Silicon dioxide (SiO_2) is used and above it micro-heater is placed.

3.3 Design parameters of micro-heater

The micro-heater design is essential for restrain the temperature distribution along the active area also to reduce power consumption. To fulfill a desired temperature distribution, user has to choose proper micro-heater geometry and substrate deliberately. This is always a key design requirement for many researchers [35,46].

Some of the basic requirements must keep in mind those are as follow:

- Material used
- Uniform temperature distribution over the heater
- Mechanical stability
- Long life
- Micro-heater geometries
- Low power consumption

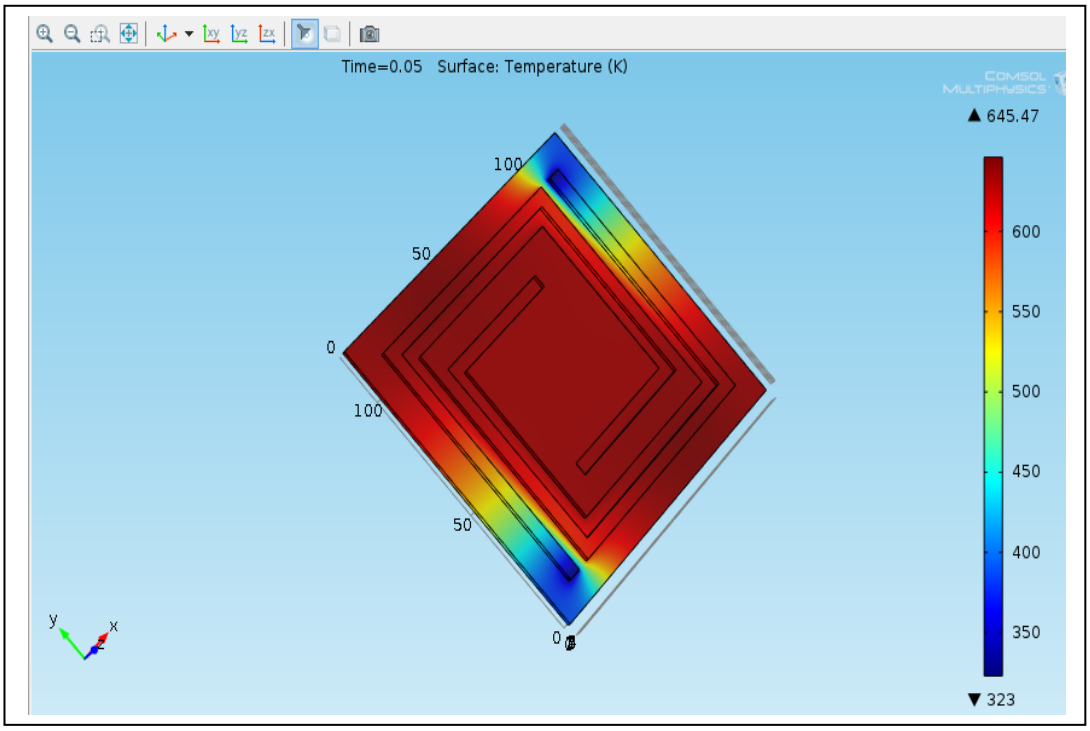

Fig 3.1 A structure of micro-heater

For most effective performance, it is a primary necessity to choose an ideal material for micro-heater. Mostly, the value of resistivity of material used micro-heater should be high. Platinum (Pt), Gallium nitride (GaN), Gallium arsenide (GaAs), Titanium nitride (TiN), DilverP1 (alloy of Ni, Co, Fe), Poly silicon (Poly-Si) and many metal alloys etc. are widely used materials for micro-heater [47].

It is essential need of micro-heater to have better temperature uniformity for proper detection of desired gases [26]. So choice of micro-heater geometry which can distribute temperature equally throughout the sensing surface area without generating any "hot spot" is desirable.

For having long life and mechanical stability of micro-heater, we should minimize stress and displacement. This is totally dependent on micro-heater material and its geometry. Also the deformation gradient and thermal expansion of micro-heater must be lower that will helpful to achieve better results.

Micro-heater geometries plays a vital role for achieve better temperature uniformity. There are many micro-heater geometries are available and are to investigated and simulated to attain uniformity.

While choosing micro-heater thickness, one should care about material strength and heat consumption of the geometry to avoid more heat dissipation loss. Preferred materials for heat (thermal) isolation are Silicon dioxide (SiO_2) and Silicon nitride (Si_3N_4). They are used as membrane under the micro-heater though Si_3N_4 is having more heat consumption than SiO_2 [31].

Low power consumption is most important parameter among all especially for battery operated sensors. As we have already seen the power consumption equation, by decreasing width and height of micro-heater geometry, we can increase resistance and that causes reduction in over all power consumption. So dimensions of micro-heater are very critical for making power efficient gas sensor.

CHAPTER-4

4.1 Selection of micro-heater material

To find micro-heater material, it is necessary to discuss material parameters such as thermal conductivity, coefficient of thermal expansion and thermal conductivity. Cooling time or heating time of micro-heater actually dependent on thermal conductivity. More the value of thermal conductivity of material, higher will be the value of rise time. Also cooling time is always marginally higher than rise time. This difference is clearly seen in metals. Variation in object size with temperature change is dependent on coefficient of thermal expansion. This is measurement of fractional change in size of structure per degree change in temperature at constant value of pressure. Lastly, electrical conductivity represents how the temperature increases due to joule heating.

It is always been a challenge to select proper material of micro-heater to achieve desired temperature requirement for any gas sensor. We have already discussed various materials available for micro-heater like, Titanium nitride (TiN), Gallium nitride (GaN), Gallium arsenide (GaAs), DilverP1 (alloy of Ni, Co, Fe), Poly silicon (Poly-Si), Platinum (Pt), and many metal alloys [47]. Among them Titanium nitride (TiN), Gallium nitride (GaN), Gallium arsenide (GaAs) are less proffered materials as they have certain major disadvantages. Dilver P1 is has many advantages such as high yield stress, low thermal power thermal expansion, low thermal conductivity but it is not that much well-known material. So for this work, Poly silicon (Poly-Si) and Platinum (Pt) are used as materials for micro-heater. Poly-Silicon (Poly-Si) has very high resistivity which makes it to more suitable for micro-heater. Whereas Platinum (Pt) has very high temperature stability (because melting point is high) so it can easily withstand at very high temperature. So micro-heater geometries are compared and analyzed using both these materials.

4.2 Micro-heater geometries and their simulation results

Various types of micro-heater geometries are simulated and analyzed using simulation tool COMSOL Multiphysics 4.3 to achieve basic two requirements namely, high temperature uniformity and low power consumptions. There are some geometries like, single meander, double meander, S-shape, fan type, spiral type etc. are chosen by researchers for making of micro-heater in metal oxide gas sensors [33,37,39].

For the simulation purpose, all geometries are made of Poly-Si with micro-heater geometry height of 2 µm and with 100 x 100 μm^2 surface area with platform of SiO_2 to provide thermal insulation to improve temperature profile [48]. And in micro-heater geometries, one end of micro-heater is having applied voltage of 3.0 V and the other end is grounded. Comparison has been made for five most desired micro-heater geometries as mentioned below.

- Single meander
- Double meander
- Fan type
- S-shape
- Spiral

The purpose of simulation of above geometry is to find the best suitable geometry which proves better temperature uniformity, so surface temperature will not be under consideration. Every simulation result represents temperature distribution by rainbow colors. Where red color area represents maximum temperature and blue area represents minimum temperature (minimum temperature is defined during boundary conditions).

Single meander geometry

Single meander geometry is simulated and result of surface temperature distribution is shown in Fig. 4.1 and Fig. 4.2, where Fig 4.1 shows the single mender geometry and Fig. 4.2 represents simulation result of temperature distribution. Simulation result displays very less temperature uniformity.

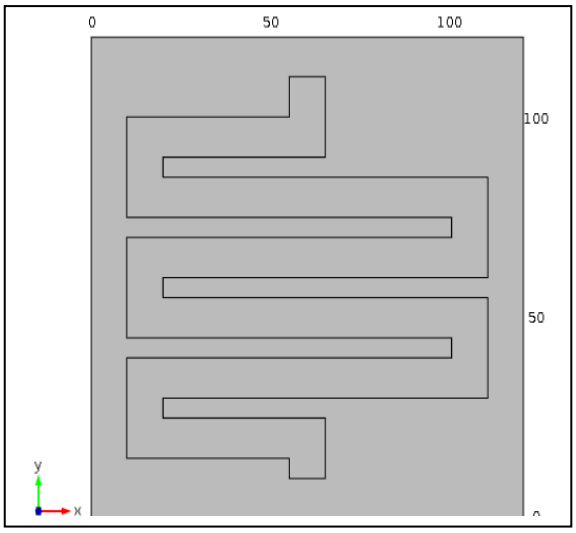

Fig. 4.1 Single Meander geometry

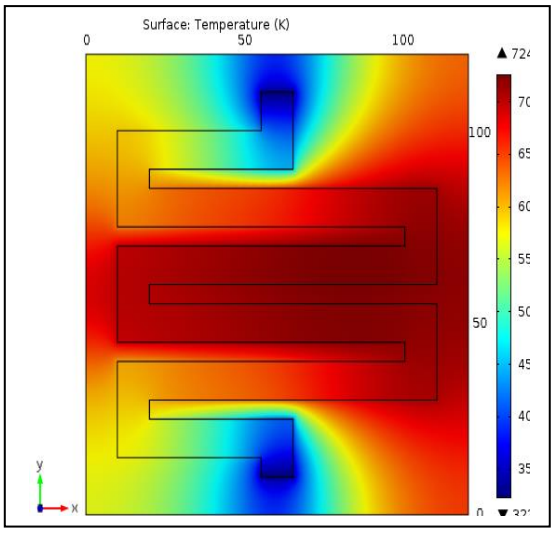

Fig. 4.2 Simulated Single Meander geometry

Double meander geometry

Single meander and double meander geometry are most studied and researched geometries among all as they are easy to fabricate and design [39]. Fig 4.3 demonstrates the single mender geometry and Fig. 4.4 shows simulation result of temperature distribution. There is a vast improvement in temperature uniformity compare with single meander geometry.

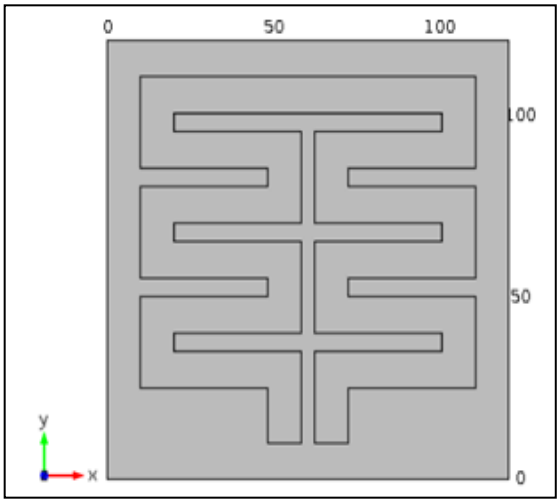

Fig. 4.3 Double Meander geometry

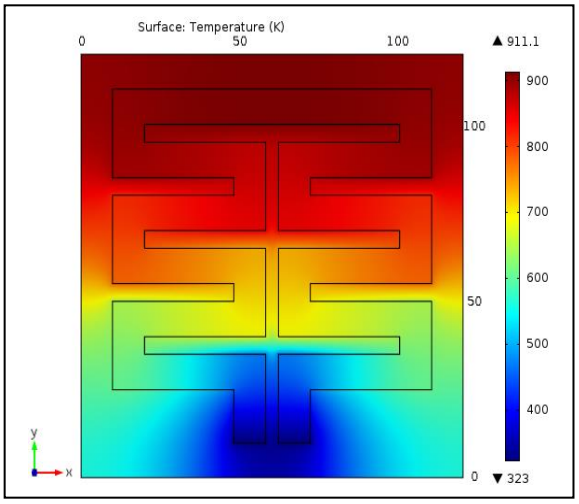

Fig. 4.4 Simulated Double Meander geometry

Fan type geometry

This type of geometry is very complicated to fabricate though it provides further improvement in temperature uniformity compare to previous discussed two geometries. Fig 4.5 is the fan type geometry and Fig. 4.6 represents simulation result.

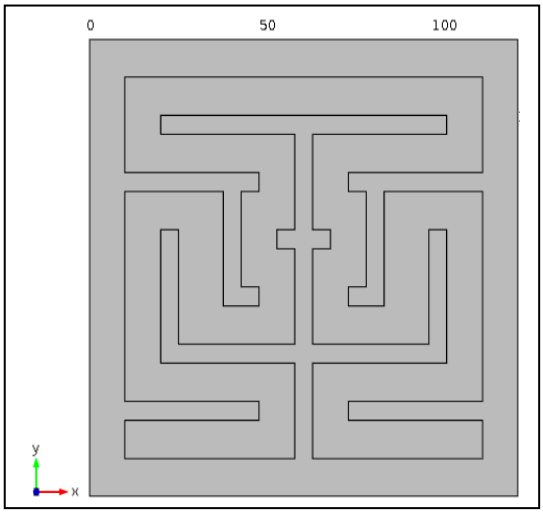

Fig. 4.5 Fan type geometry

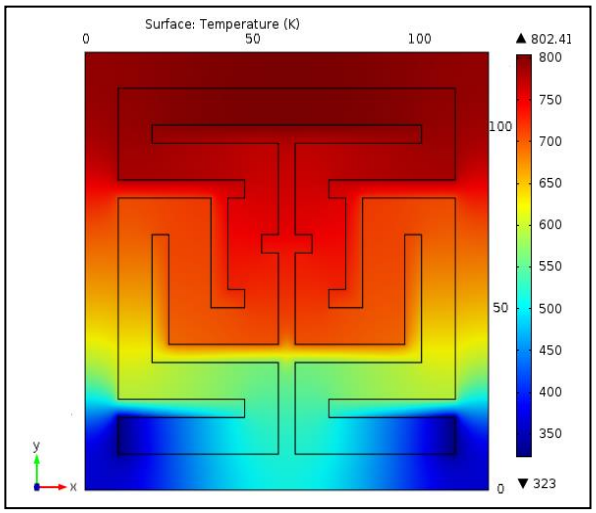

Fig. 4.6 Simulated Fan type geometry

S-shape geometry

This geometry has more material deposition at the central part. So it is observed in result that there is more temperature and higher uniformity in the geometry. But these type of geometries have problem of high stress due to thermal expansion [37]. Fig. 4.8 is a simulation result of S-shape geometry where it can be observed that it has greater uniformity.

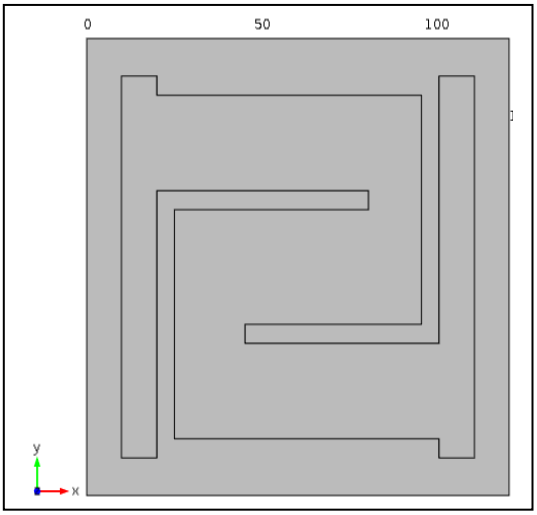

Fig. 4.7 S-shape geometry

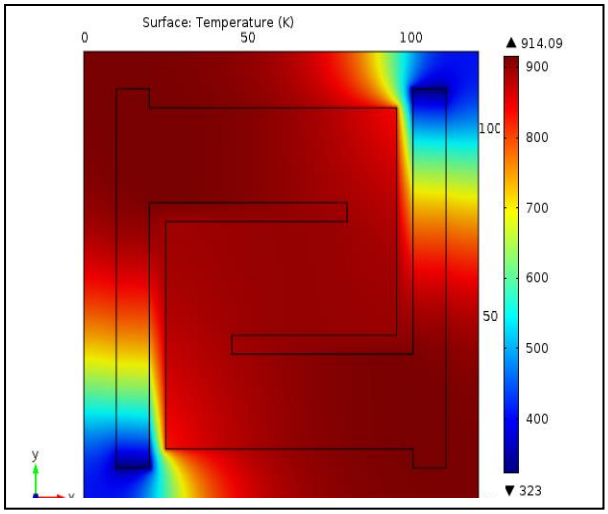

Fig. 4.8 Simulated S-type geometry

Spiral geometry

S-shape geometry has better surface temperature uniformity though that has some drawbacks also. Spiral geometry is best solution for micro-heater geometry (Fig. 4.10) among above mentioned geometries. It has also low power consumption than S-shape geometry and has more area under the heat [36].

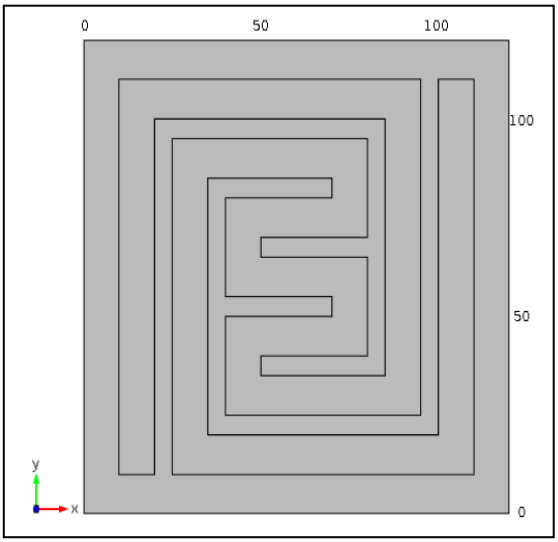

Fig. 4.9 Spiral geometry

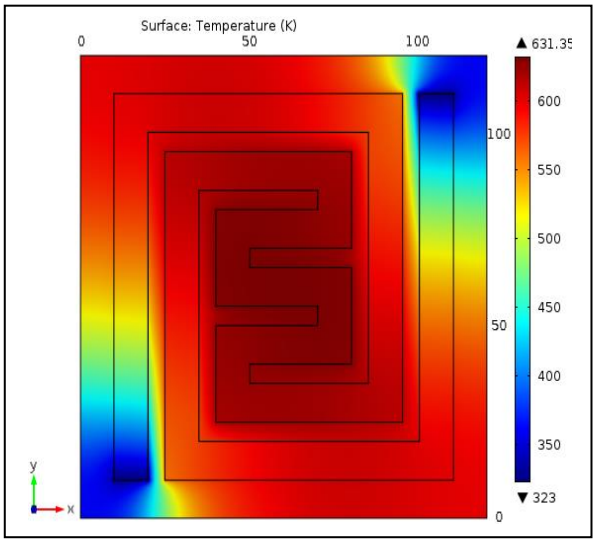

Fig. 4.10 Simulated Spiral geometry

There may be further improvement in result possible by making edges of geometries curved. This will improve mechanical stability, minimum edge losses and improvement in maximum surface temperature of micro-heater geometries.

Modified Spiral geometry

There is a further change of temperature uniformity in the same spiral geometry by merging central area or in other word more deposition in middle portion of geometry. Geometry will be seen like shown in Fig. 4.11 and micro-heater exhibit more temperature uniformity then simple spiral geometry (Fig. 4.10).

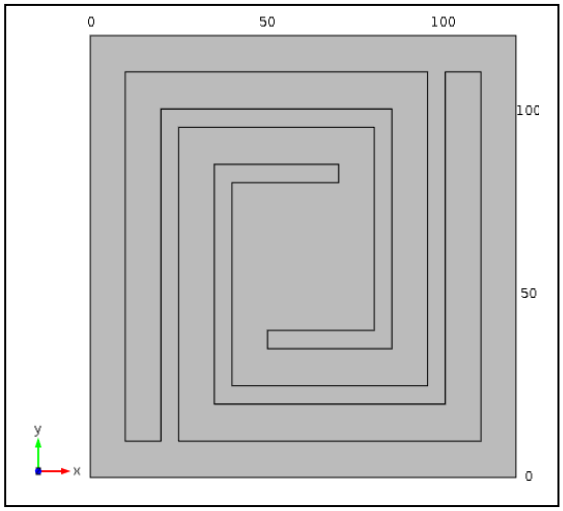

Fig. 4.11 Modified Spiral geometry

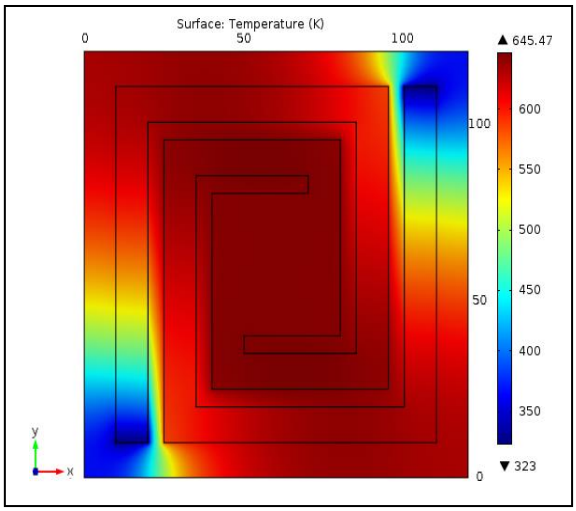

Fig. 4.12 Simulated Modified Spiral geometry

4.3 Conclusion

It is always desirable to have better surface temperature of sensing surface (which is delivered by micro-heater) for correct detection of certain gases. We have simulated various micro-heater geometries but S-shape, spiral and modified spiral geometries provides good surface temperature uniformity. S-shape geometry has high stress and less stability at high temperature as more deposition in middle portion of geometry. Also spiral geometry is next available option for micro-heater as it has better result of temperature uniformity compare to single meander, double meander and fan type geometries. That can be also improvised by modifying central area of micro-heater. So we have best available solution of present time micro-heater geometry as modified spiral geometry.

In the next chapter, we will simulate this modified spiral micro-heater geometry by using Platinum and Poly-Si as micro-heater material. We will see distribution of current density on the surface, stress on surface, temperature uniformity on surface, power consumption and micro-heater transient response time for both the cases (Platinum and Poly-Si). Furthermore, we will discuss effect of height (thickness) variation on power consumption and temperature of micro-heater. Also there will be discussion on width variation of micro-heater geometry and its effect on temperature uniformity. All results will be compared and conclusion will be made based on these.

CHAPTER-5

5.1 Parameters consideration under electro – thermal analysis

During the simulation and result analysis, some parameters of micro-heater are considered as most crucial as they directly affect the performance of gas sensor. They are mentioned below:

- Maximum temperature
- Temperature uniformity
- Power consumption
- Transient temperature response
- Transient resistance response of micro-heater
- Current density

We have already discussed parameters like, maximum temperature, temperature uniformity and power consumption so they are not deliberated further in discussion. As response / recovery time of gas sensor is dependent on sensing surface temperature and sensing surface temperature is relied on transient temperature response of micro-heater, it is more crucial to have minimum transient temperature response time of micro-heater. Due to joule-heating there is variation in resistance of micro-heater. As temperature increases, value of resistance raises. Also current density represents the distribution of current on the micro-heater surface (current / area).

5.2 Electro-Thermal analysis

In the previous chapter, various geometries are tried and analyzed for optimum solution of micro-heater geometry. Then modified spiral geometry is found as optimum solution which having high resistance value (which is helpful for resistive heating) and less power consumption. We have already discussed resistive heating (Q) equation in chapter 2 that is,

$$Q = \sigma \cdot |\nabla V|^2 \tag{5.1}$$

For particular temperature range, the electric conductivity σ is a function of temperature T according to:

$$\sigma = \frac{\sigma_0}{1+\alpha\left(T - T_0\right)} \tag{5.2}$$

Where α is the temperature coefficient of resistivity, which describes how the resistivity varies with temperature and σ_0 is the conductivity at the reference temperature T_0. Also we know that the basic resistance equation including cross sectional area A is,

$$R = \frac{\rho \cdot l}{A}$$
$$= \frac{l}{\sigma \cdot A} \tag{5.3}$$

From above equation, electric conductivity σ and cross sectional area A are inversely proportional. Also from equation (1), we can conclude that either increases the voltage gradient of micro-heater two ends (simply increases applied voltage potential of electrode) or increases the area (thickness or width) of micro-heater. Let us discuss two cases in which variations in voltage gradient and variations in thickness / area (thickness * width = area) of micro-heater geometry is analyzed for measure changes in temperature and power consumption of micro-heater.

Case 1: Change the applied voltage for constant dimensions of micro-heater geometry.

Case 2: Change the thickness of micro-heater geometry for constant applied voltage.

Modified spiral geometry which is shown in Fig. 5.2.1, is having 2 µm thickness and it is placed on 120 x 120 μm^2 insulating platform of SiO_2 having 2 µm thickness. All dimensions are shown in Fig. 5.2.2. It is analyzed using COMSOL Multiphysics 4.3. Properties of SiO_2 and Poly-Si are defined in **Appendix 1**. As shown in Fig. 5.2.2, micro-heater has equal stripe area of 10 µm except the central area of the geometry and central area is of 40 x 40 μm^2.

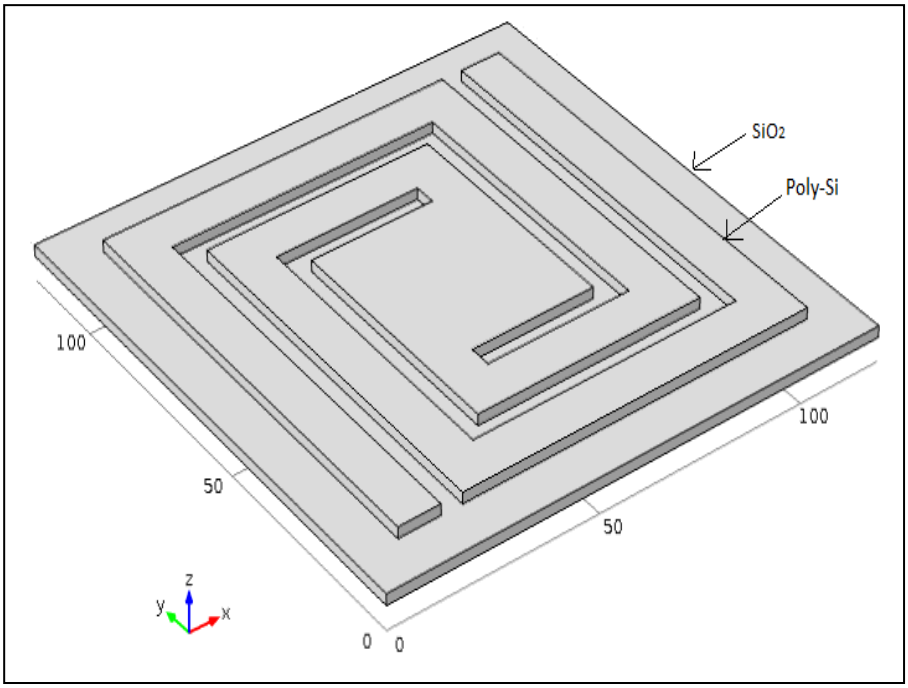

Fig. 5.2.1 3D view of Poly-Si based modified spiral geometry

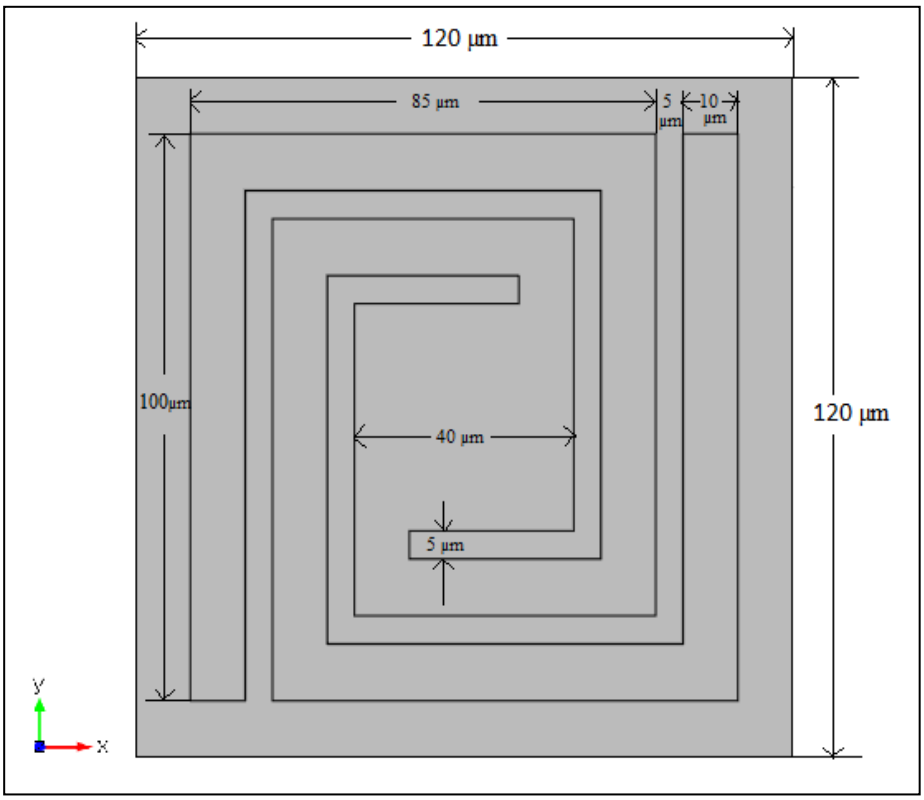

Fig. 5.2.2 2D view of modified spiral geometry with dimensions

Our aim is to generate surface temperature around 640 - 650K for the analysis of both the cases.

Case 1: Change the applied voltage for constant dimensions of micro-heater geometry

In this case, modified spiral geometry is examined by varying applied voltage from 0 V to 3.0 V and surface temperature variation is observed. Relation between applied voltage and maximum temperature is as shown in Fig. 5.2.3. As explained in equation (1) heat generated is proportional with square of the voltage gradient, result also reflects non-linear relationship between applied voltage and maximum surface temperature. Result shows the variations in maximum temperature start from 323° K to 645.47° K for given applied voltage from 0 V to 3.0 V. It can be observed that temperature variation occurs during the period 0 V to 1.5 V is from 323.0° K to 415.0° K which is quite less as compare with the period 1.5 V to 3.0 V which is from 415.0° K to 645.47° K. Increment in voltage gradient implies non-linear increment in maximum surface temperature.

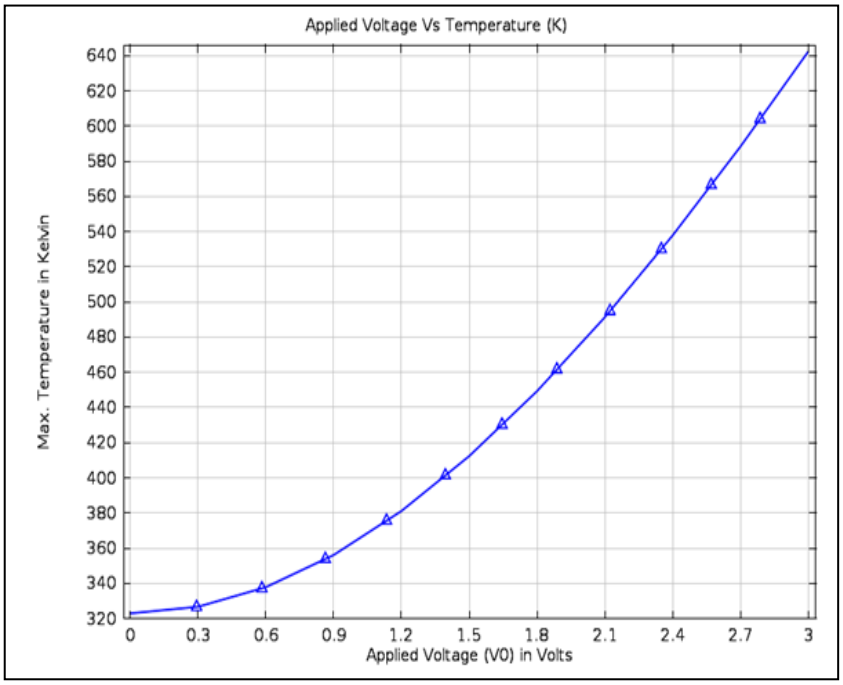

Fig. 5.2.3 Maximum temperature with variations in applied voltages for Poly-Si based micro-heater

Case 2: Change the thickness of micro-heater geometry for constant applied voltage

Cross sectional area *A* or thickness of micro-heater also affects resistive heating (equation (1) and equation (3)). Consider constant applied voltage of 3.0 V and thickness of micro-heater geometry is varied from 1 µm to 2 µm for same stripe width. Variations in maximum temperature with thickness of micro-heater geometry are measured and characterized as shown in Fig. 5.2.4.

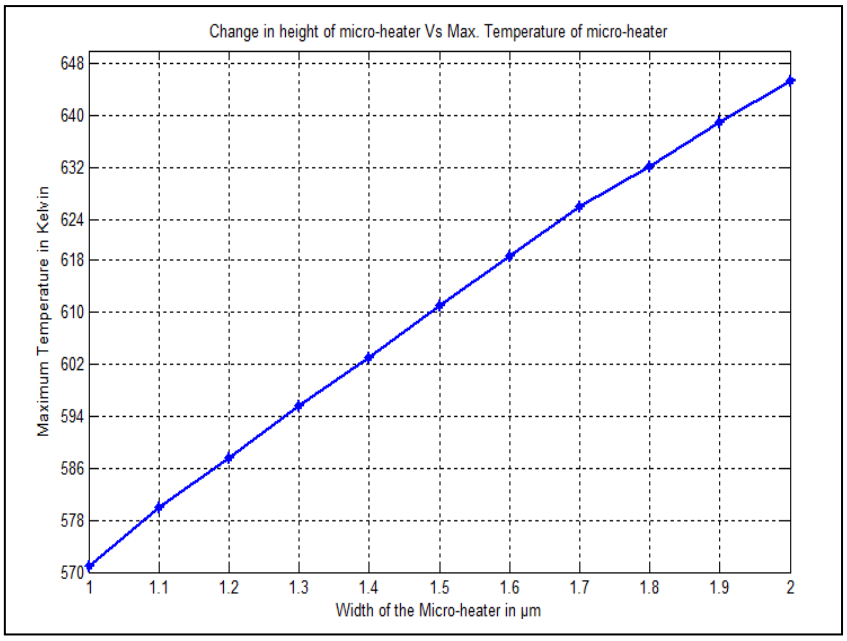

Fig. 5.2.4 Change in thickness Vs maximum temperature characteristic

It can be analyzed that there is almost linear relation between thickness variation and maximum temperature of micro-heater. As thickness of micro-heater varies from 1 µm to 2 µm, maximum temperature varies from to 645.47° K with almost equal change throughout the thickness variation. As thickness increases, resistance of micro-heater reduces that leads to increase in power consumption. Also transient temperature response time is also rising with enlargement in thickness of micro-heater. Table 5.2.1

Table 5.2.1 Effect of thickness variation of micro-heater on other parameters for Poly-Si

Sr. No.	**Thickness of micro-heater geometry**	**Max. Temp**	**Power Consumption**	**Resistance value**	**Transient temperature response**
	µm	**K**	**mW**	**Ω**	**ms**
1.	1.0	570.96	6.55	1375	11.5
2.	1.2	587.56	7.78	1156.8	12.53
3.	1.4	602.9	8.98	998.34	13.56
4.	1.6	618.42	10.21	880.53	14.6
5.	1.8	632.2	11.42	787.41	15.62
6.	2.0	645.47	12.63	713	16.66

From the Table 5.2.1, it is clear that thickness of micro-heater geometry affect maximum temperature, power consumption, resistance of micro-heater and transient

temperature response. Except resistance of micro-heater, all the parameters will increase with increase in thickness of micro-heater geometry.

5.3 Effect of width variation in micro-heater geometry

We have already understood **case 2** where increment in thickness of micro-heater causes change in parameters. Also we have discussed that heat capacity dependent on area (i.e. thickness and width). Now consider double meander geometry having 2 µm thickness of micro-heater geometry and SiO_2 based insulating platform of 120 x 120 μm^2 and 2 µm thickness.

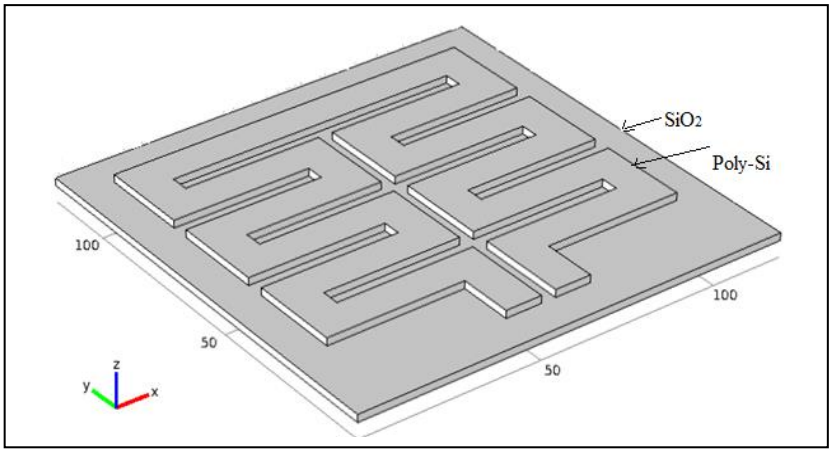

Fig. 5.3.1 3D view of double meander geometry

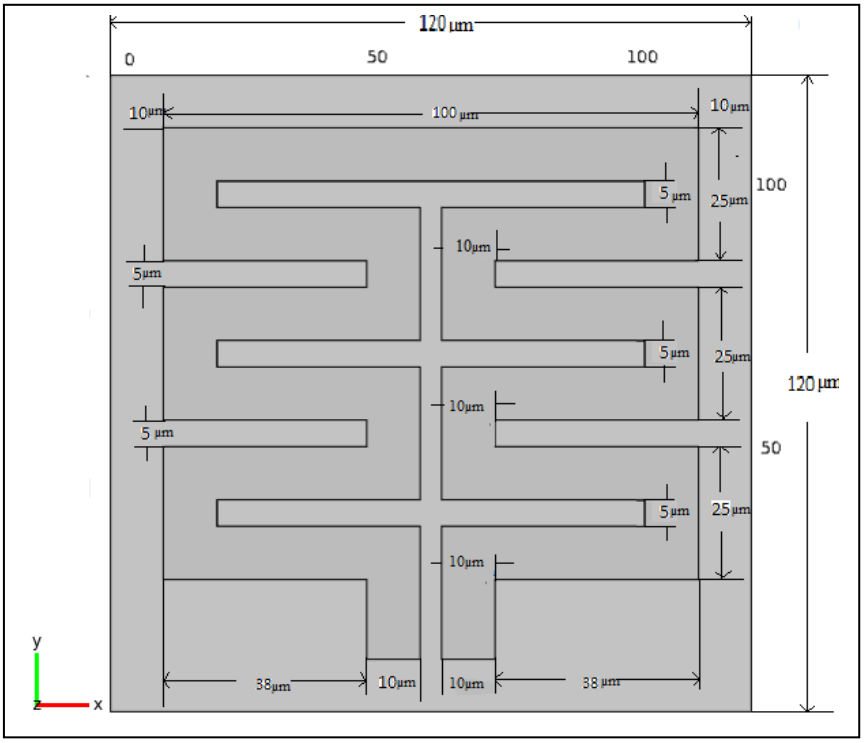

Fig. 5.3.2 2D view of double meander geometry with dimensions

We are going to change its width and we will analyze the effect on surface temperature. Fig. 5.3.1 shows double meander geometry and Fig. 5.3.2 shows same geometry with dimensions.

Now structure widths are varied as shown in Fig. 5.3.3 and Fig. 5.3.4. Simulation result of double meander geometry and changed width double meander geometry are compared in Fig. 5.3.5 and Fig. 5.3.6 respectively.

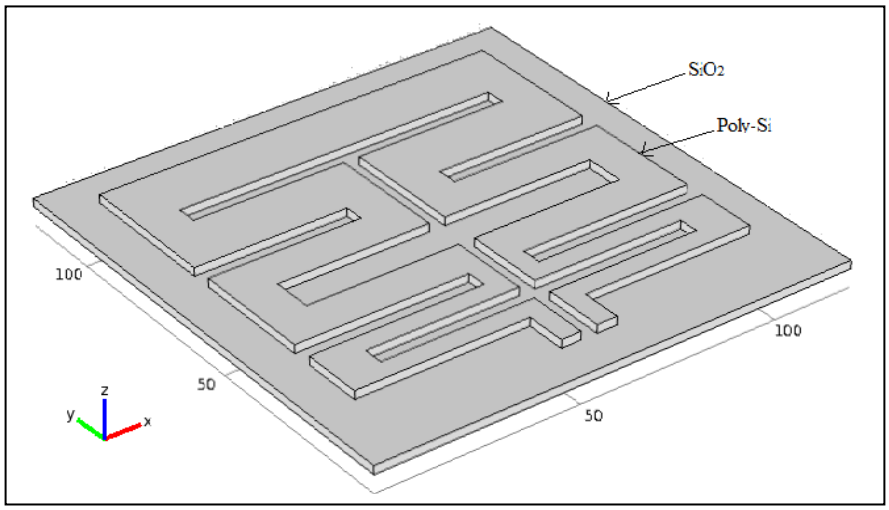

Fig. 5.3.3 3D view of changed width double meander geometry

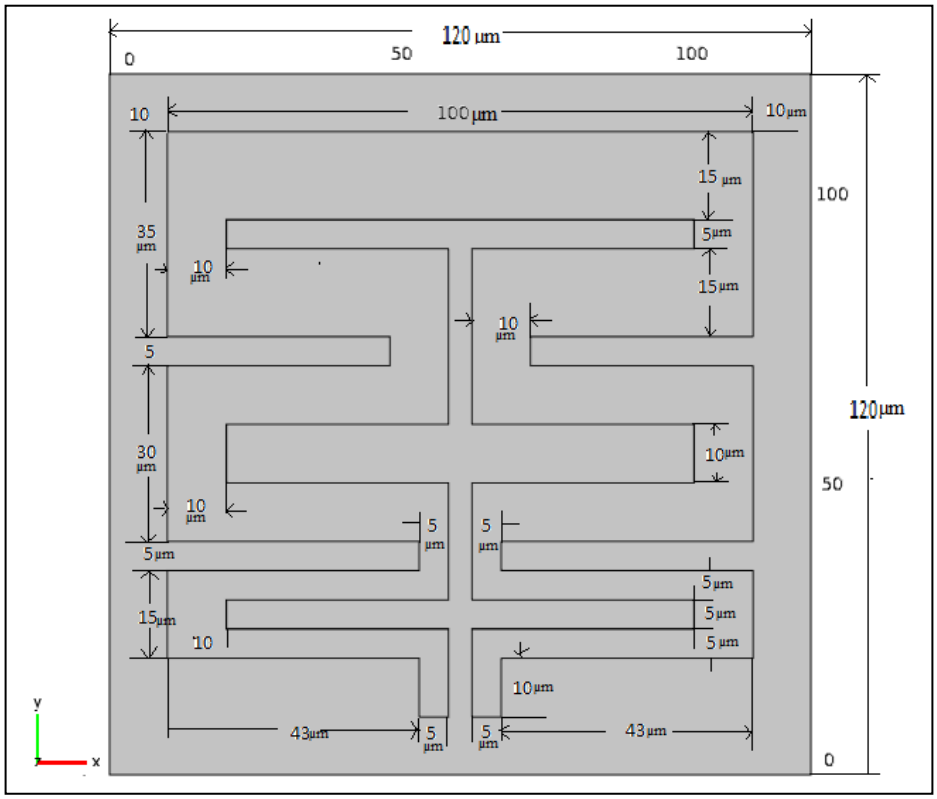

Fig. 5.3.4 2D view of Poly-Si based changed width double meander geometry with dimensions

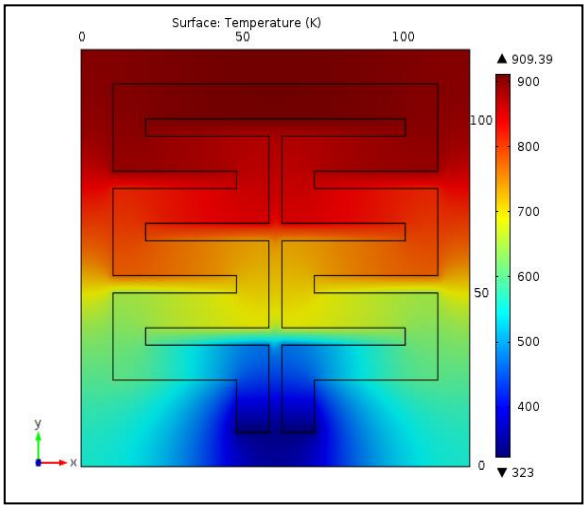

Fig. 5.3.5 Simulated result for double meander geometry

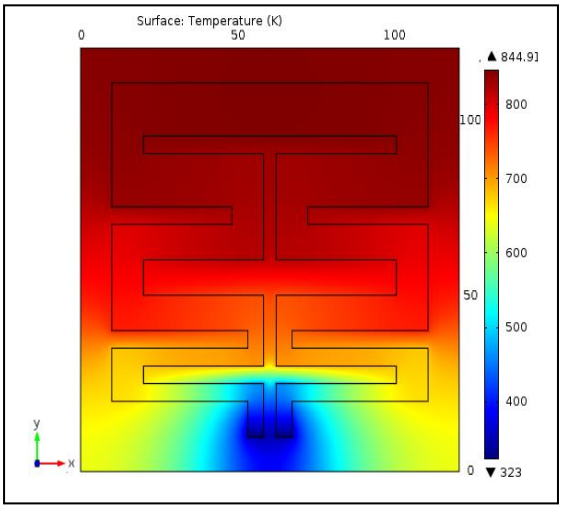

Fig. 5.3.6 Simulated result for changed width double meander geometry

If we reduce the cross sectional area (width) at which less temperature and increases area at which we have high temperature better temperature uniformity can be achieved as shown in Fig. 5.3.5 and Fig. 5.3.6.

5.4 Simulation of Poly-Si based modified spiral geometry

As we have already seen the modified spiral geometry in Fig. 5.2.1, we are going to applied 3.0 V supply voltage at one electrode of geometry, 2 µm is thickness of geometry, and SiO_2 based insulating platform of 120 x 120 μm^2 and 2 µm thickness. We are trying to find different parameters of this geometry. Fig. 5.4.1 represents surface temperature response.

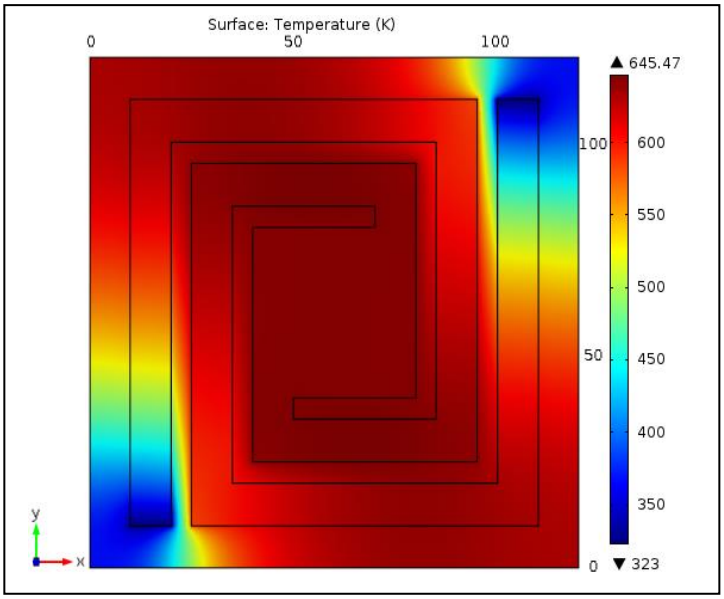

Fig. 5.4.1 Simulated Poly-Si based modified spiral geometry

Its current density is simulated and response is shown in Fig.5.4.2. There is maximum current density at the corner edges and minimum current density at center.

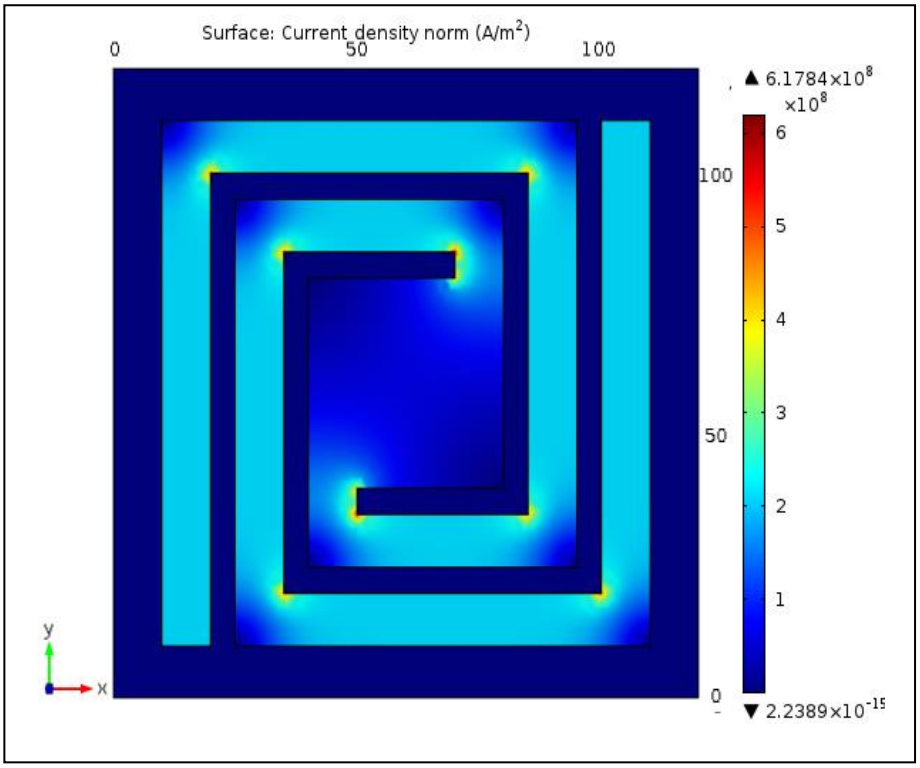

Fig. 5.4.2 Current density of Poly-Si based modified spiral geometry

Its transient resistance response, transient temperature response and transient power consumption is simulated and Fig. 5.4.3, Fig. 5.4.4 and Fig. 5.4.5 represent all three responses respectively.

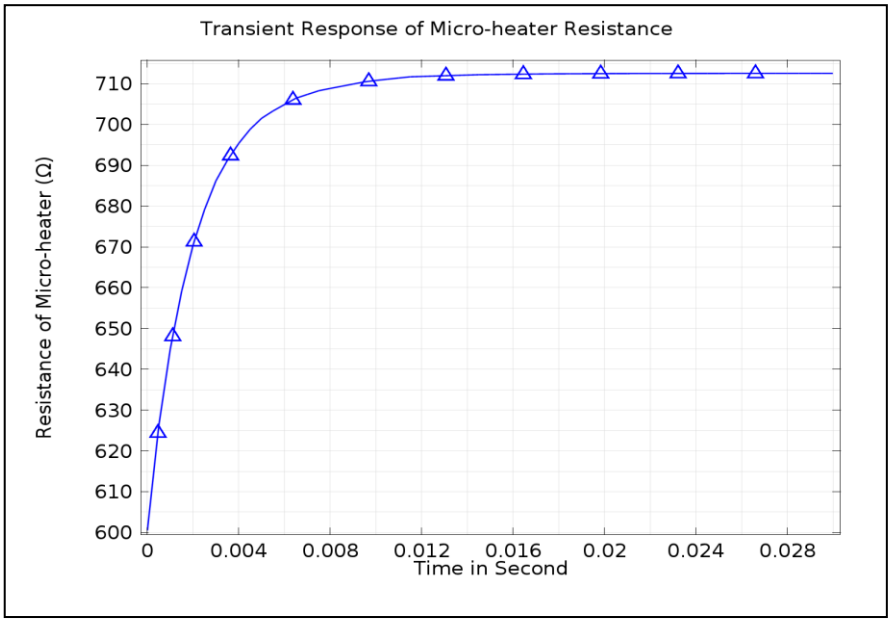

Fig. 5.4.3 Transient response of resistance of Poly-Si based modified spiral geometry

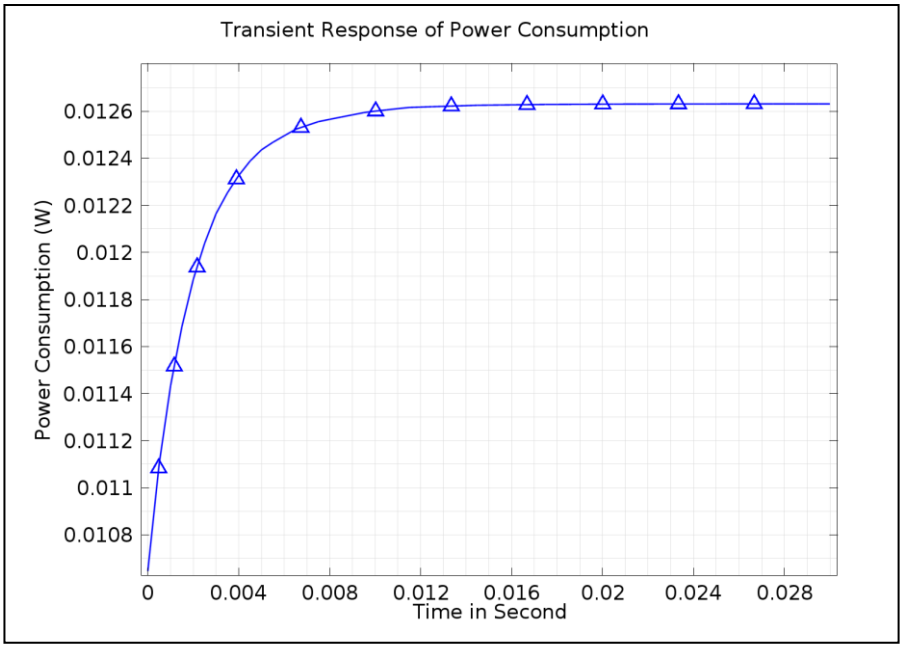

Fig. 5.4.4 Transient response of power consumption of Poly-Si based modified spiral geometry

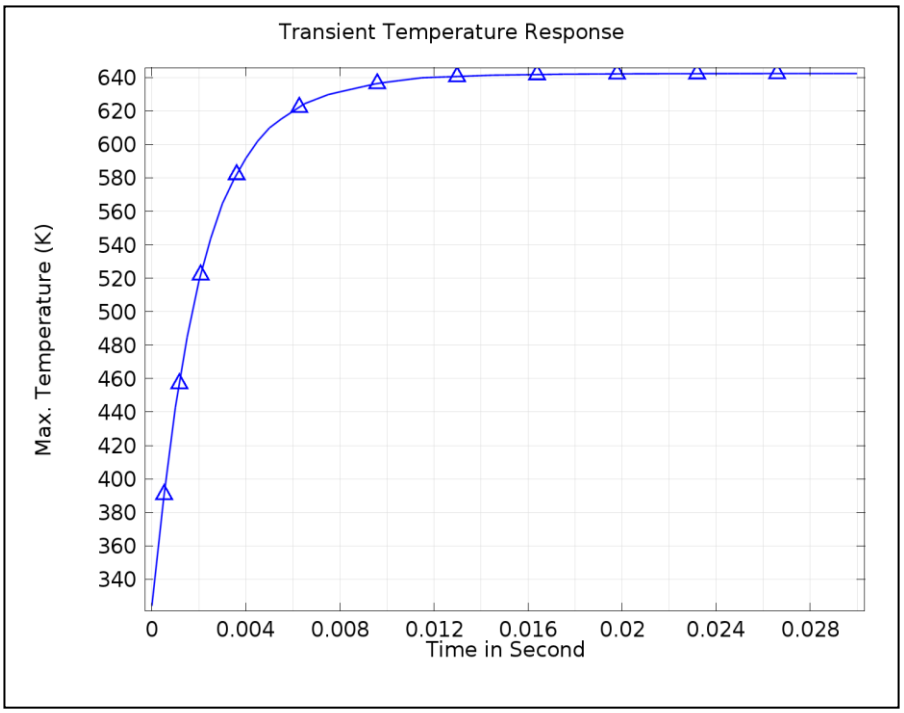

Fig. 5.4.5 Transient temperature response of Poly-Si based modified spiral geometry

Now, we will change the geometry and trying to improve results for better temperature uniformity. So we are changing the width of geometry accordingly. Fig. 5.4.6 and Fig. 5.4.7 shows changed width geometry for better temperature uniformity. We will inspect other parameters like, current density, transient resistance response, transient temperature response and transient power consumption also.

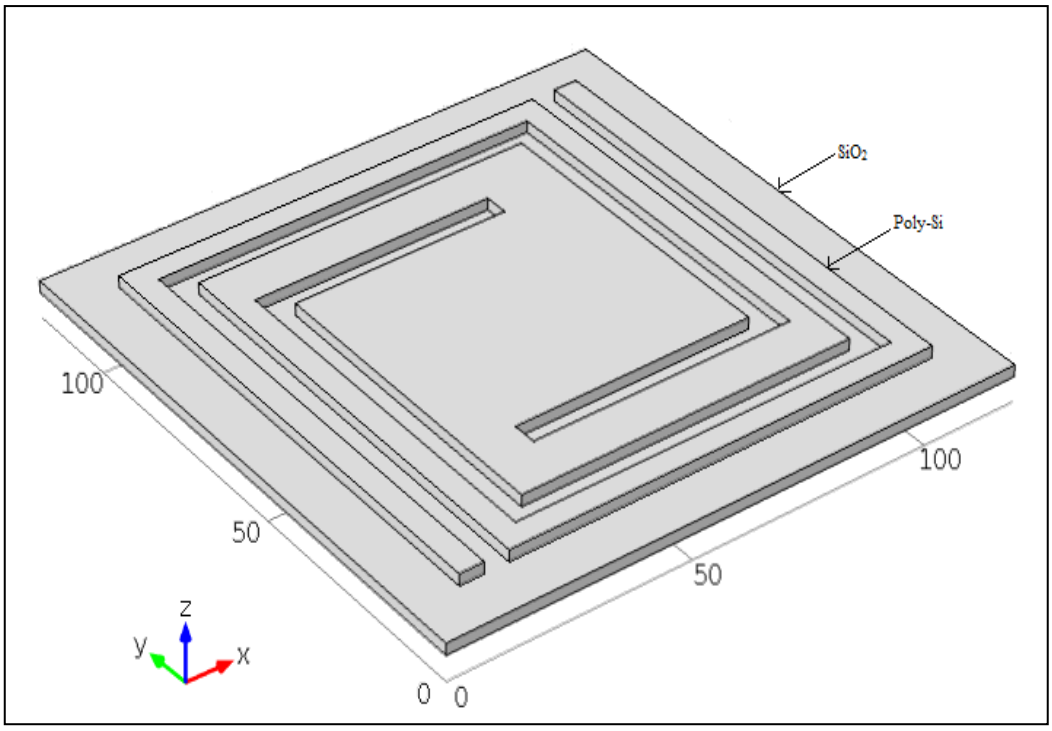

Fig. 5.4.6 3D view of Poly-Si based changed width modified spiral geometry

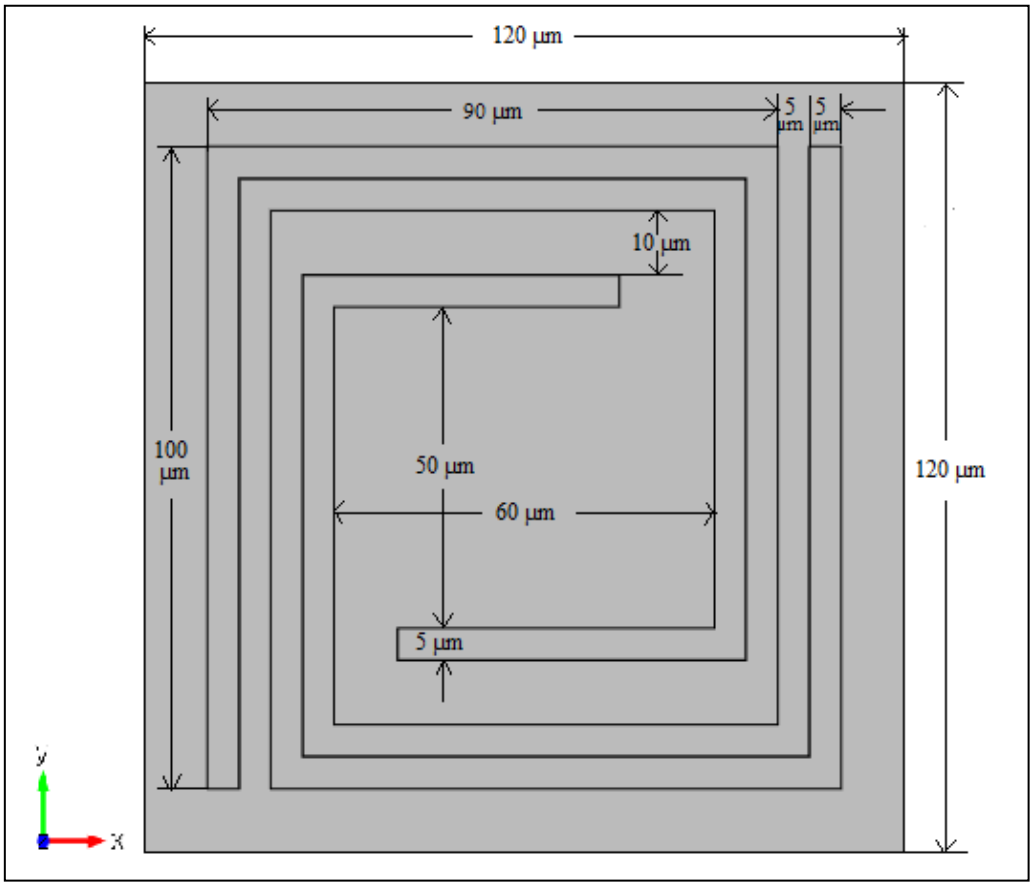

Fig. 5.4.7 2D view with dimensions of Poly-Si based changed width modified spiral geometry

After simulation, we have better temperature uniformity on micro-heater geometry as shown Fig. 5.4.8. After comparison of result Fig. 5.4.1 and Fig. 5.4.8, we can conclude that after proper width variation, we can improve temperature uniformity.

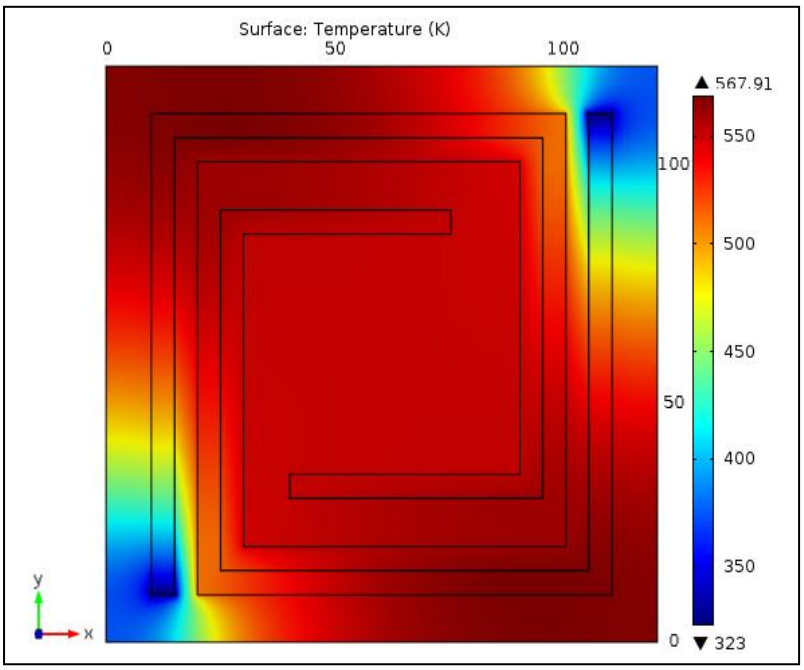

Fig. 5.4.8 Simulated Poly-Si based changed width modified spiral geometry

Also Fig. 5.4.9, Fig.5.4.10, Fig. 5.4.11 and Fig. 5.4.12 are shown below; they are responses of current density, transient resistance response, transient temperature response and transient power consumption respectively.

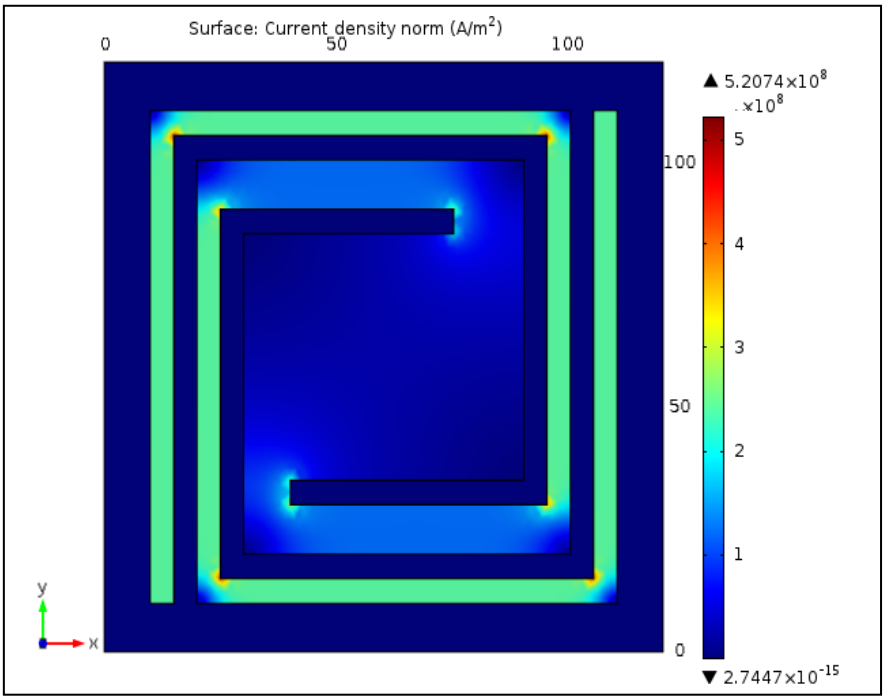

Fig. 5.4.9 Current density of Poly-Si based changed width modified spiral geometry

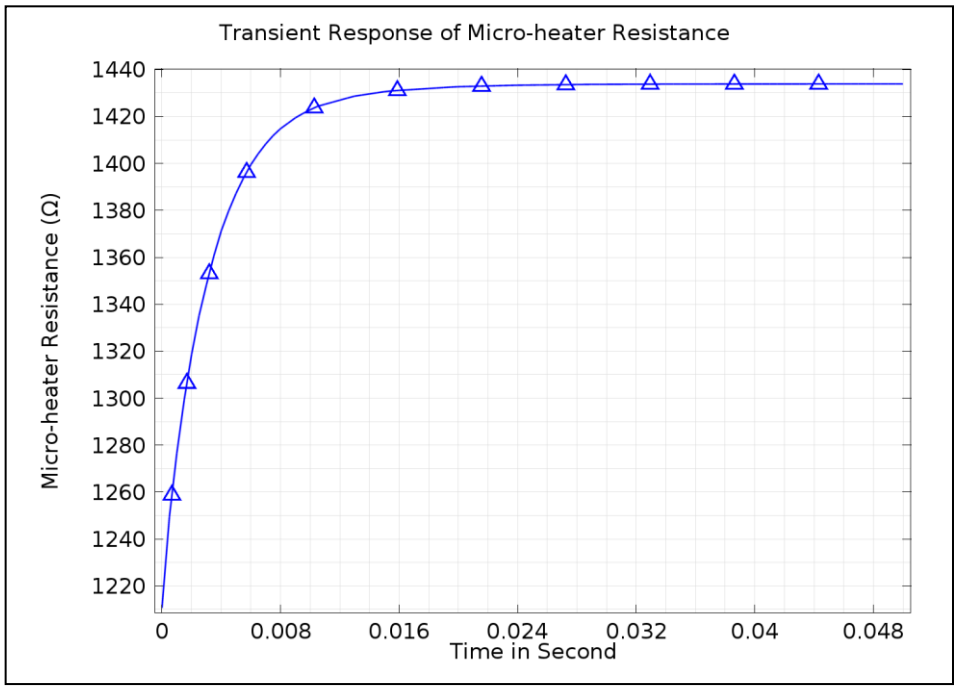

Fig. 5.4.10 Transient response of resistance of Poly-Si based changed width modified spiral geometry

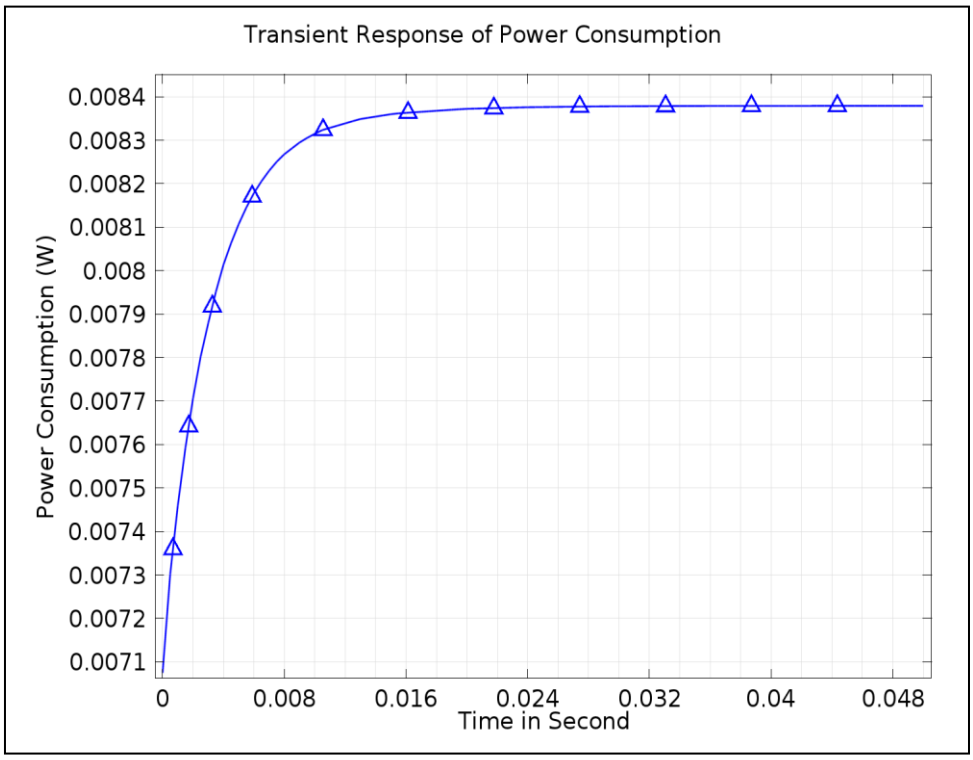

Fig. 5.4.11 Transient response of power consumption of Poly-Si based changed width modified spiral geometry

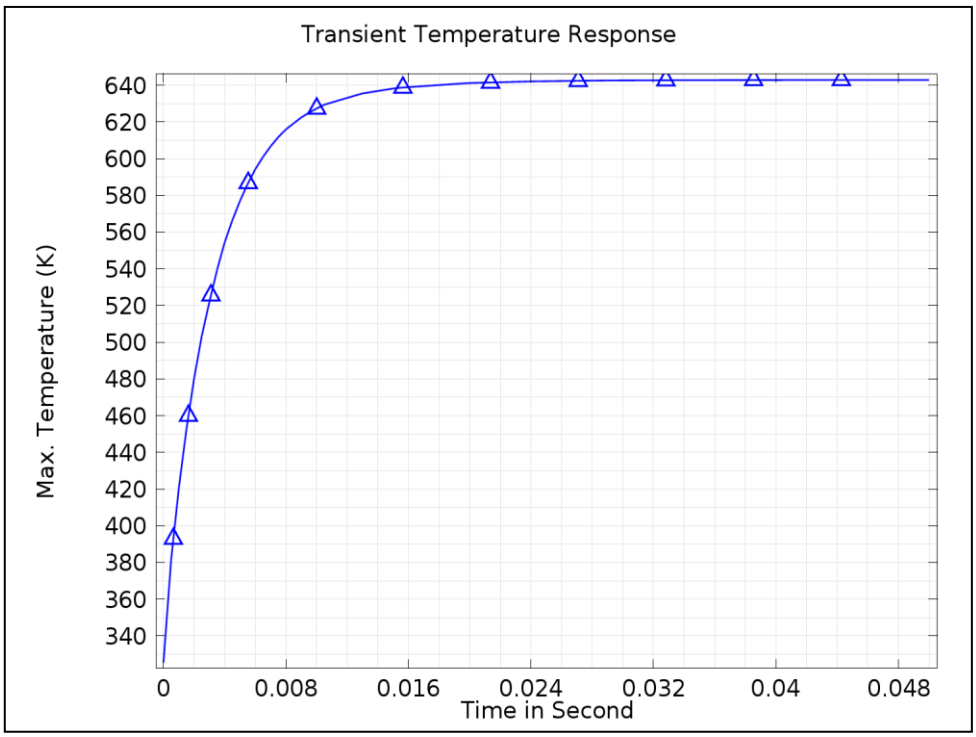

Fig. 5.4.12 Transient temperature response of Poly-Si based changed width modified spiral geometry

Results are compared for both the Poly-Si based geometries and shown in Table 5.4.1.

Table 5.4.1 Comparison of parameters of two geometries for Poly-Si

	Spiral Geometry with equal width of 10µm	**Spiral Geometry with unequal width**
Max. Surface Temperature	645.47 °K at 3.0V	572.89 °K at 3.0V 645.47 °K at 3.4662V
Transient Temperature response time	13 ms	23 ms
Resistance Variation	600.51 Ω to 712.54 Ω (till temperature reaches 323 °K to 645.47 °K)	1210.6 Ω to 1433.8 Ω (till temperature reaches 323 °K to 645.47 °K)
Power Consumption	12.63mW	8.3791mW

5.5 Simulation of Platinum based modified spiral geometry

As now, we are known with modified spiral geometry as shown in Fig. 5.2.1. But in this case, platinum based micro-heater is placed on SiO_2 platform of 120 x 120 μm^2 surface. Properties of Platinum are defined in **Appendix 1**. It is observed that around 640-650^o K temperature is achieved at only 0.3V supply. Simulation result is shown in Fig. 5.5.1.

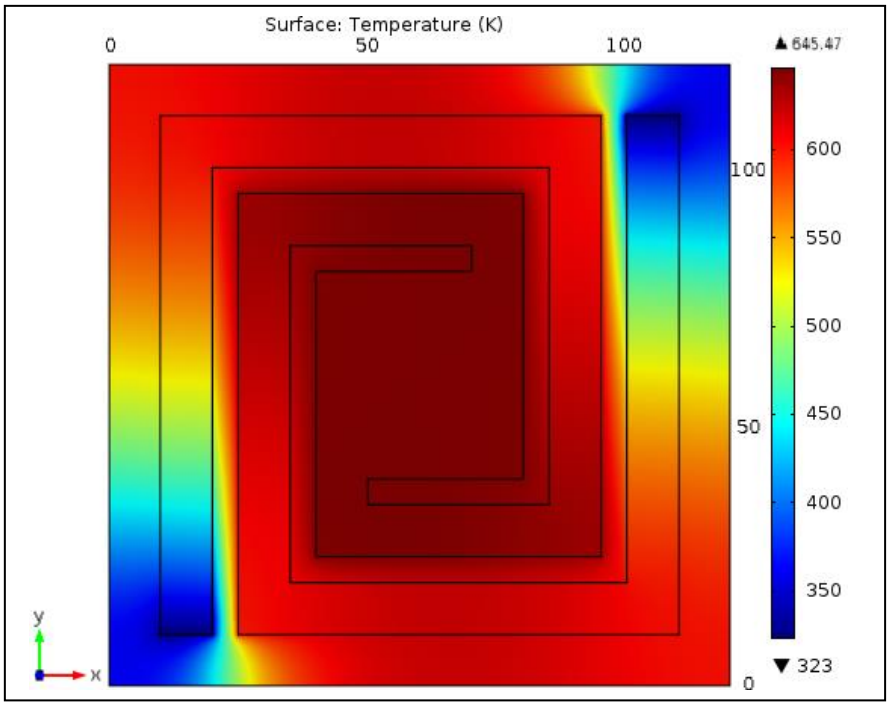

Fig. 5.5.1 Simulated Platinum based modified Spiral geometry

As we have considered two cases in Poly-Si based micro-heater geometry, same cases are taken for Platinum based geometry.

Case 1: Change the applied voltage for constant dimensions of micro-heater geometry

In joule heating example, it was discussed that heating is proportional to square of voltage gradient. Applied voltage is varied from 0 V to 0.3 V for Platinum based micro-heater and result is analyzed. We can observe that variation from 0 V to 0.15 V, there is maximum surface temperature variation is from 323^o K to 428^o K. As voltage gradient is more from 0.15 V to 0.3 V, we have temperature variation from 428^o K to

645.47° K. (large temperature variation can be observed). So graph shown in Fig. 5.5.2 is non-linear.

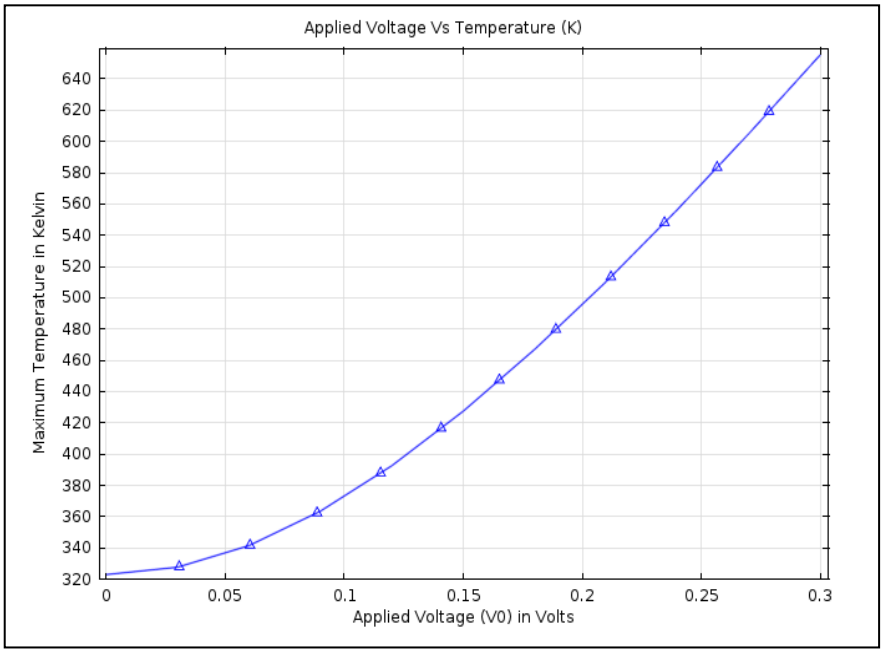

Fig. 5.5.2 Maximum temperature with variations in applied voltages for Platinum based micro-heater

Now consider 2nd case where we will observe change in parameter with thickness variation.

Case 2: Change the thickness of micro-heater geometry for constant applied voltage

Consider modified micro-heater geometry and varied its thickness from 1 µm to 2 µm for constant applied voltage of 0.3V. Fig. 5.5.3 shows response of thickness variation and maximum surface temperature which is almost linear.

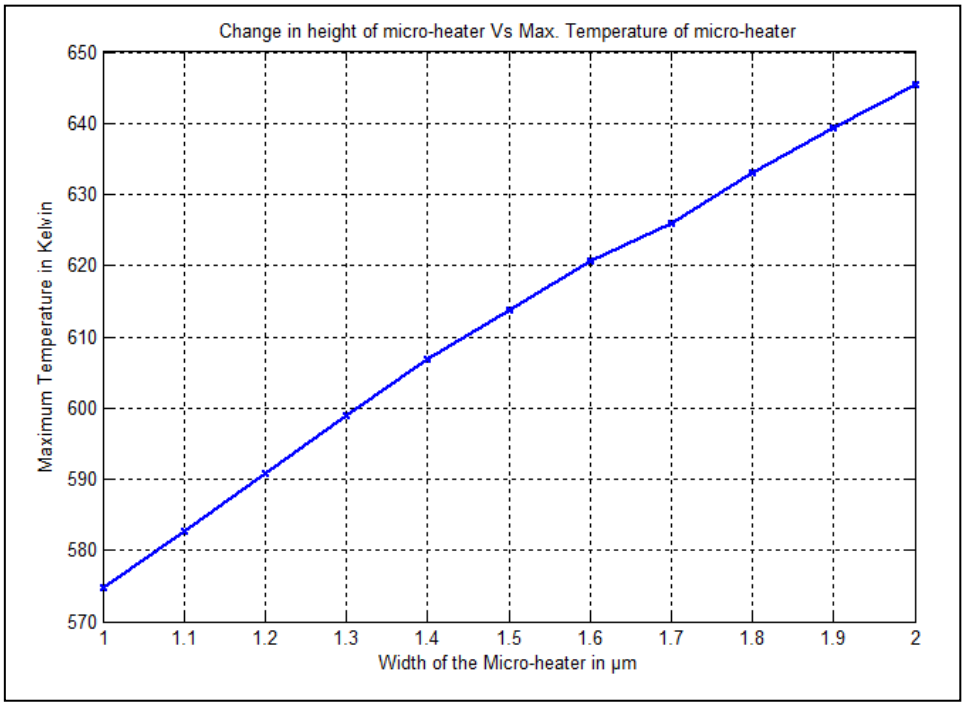

Fig. 5.5.3 Change in thickness Vs maximum temperature characteristic

Also Table 5.5.1 represents effect of thickness variation of micro-heater on other parameters like, maximum temperature of surface, power consumption of micro-heater, resistance of micro-heater and transient response time. It is observed that with thickness increases, maximum temperature of surface increases, power consumption increases, resistance of micro-heater decreases and transient temperature response time increases.

Table 5.5.1 Effect of thickness variation of micro-heater on other parameters for Platinum

Sr. No.	Thickness of micro-heater geometry	Max. Temp	Power Consumption	Resistance value	Transient temperature response
	μm	K	mW	Ω	ms
1.	1.0	574.71	10	9.02	13.82
2.	1.2	590.76	11.8	7.62	14.31
3.	1.4	606.77	13.52	6.63	14.84
4.	1.6	620.61	15.48	5.88	15.32
5.	1.8	633.1	17.05	5.28	15.8
6.	2.0	645.47	18.83	4.79	16.35

Its current density is simulated and response is shown in Fig.5.5.4. At the corner edges, we have maximum current density.

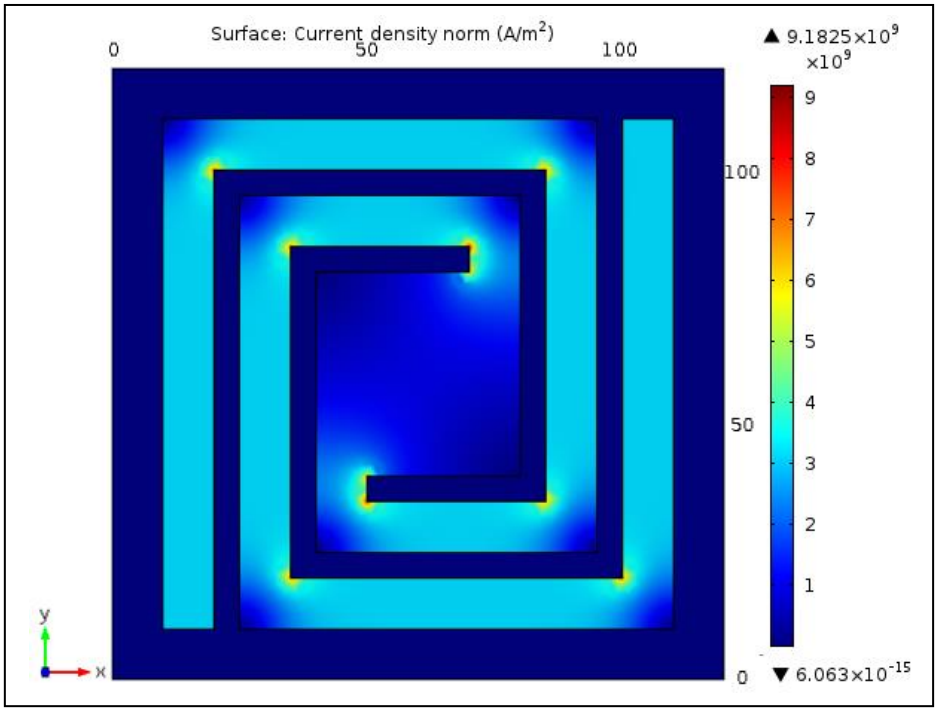

Fig. 5.5.4 Current density of Platinum based modified spiral geometry

Fig. 5.5.5, Fig. 5.5.6 and Fig. 5.5.7 are represented by transient resistance response, transient power consumption response and transient temperature response respectively.

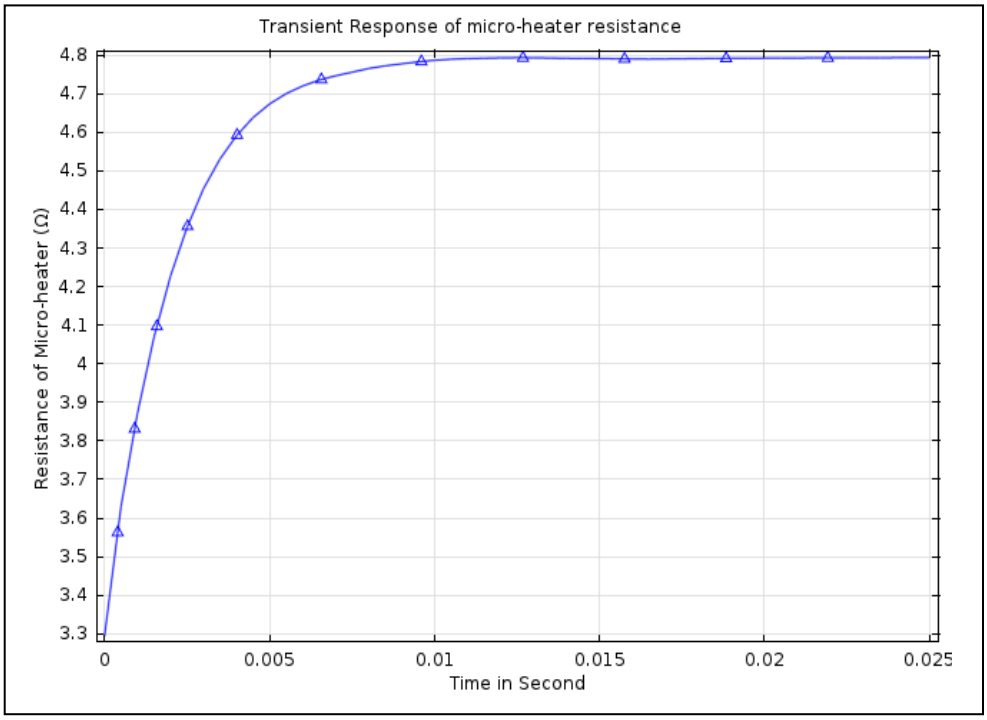

Fig. 5.5.5 Transient response of Platinum based micro-heater resistance

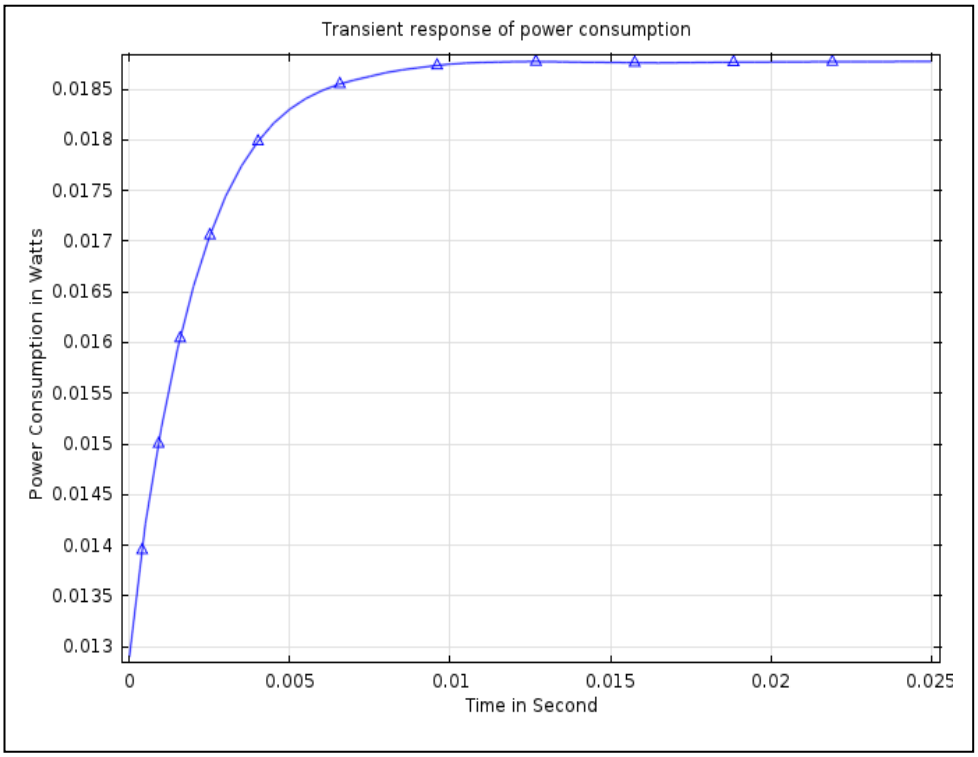

Fig. 5.5.6 Transient response of power consumption of Platinum based modified spiral geometry

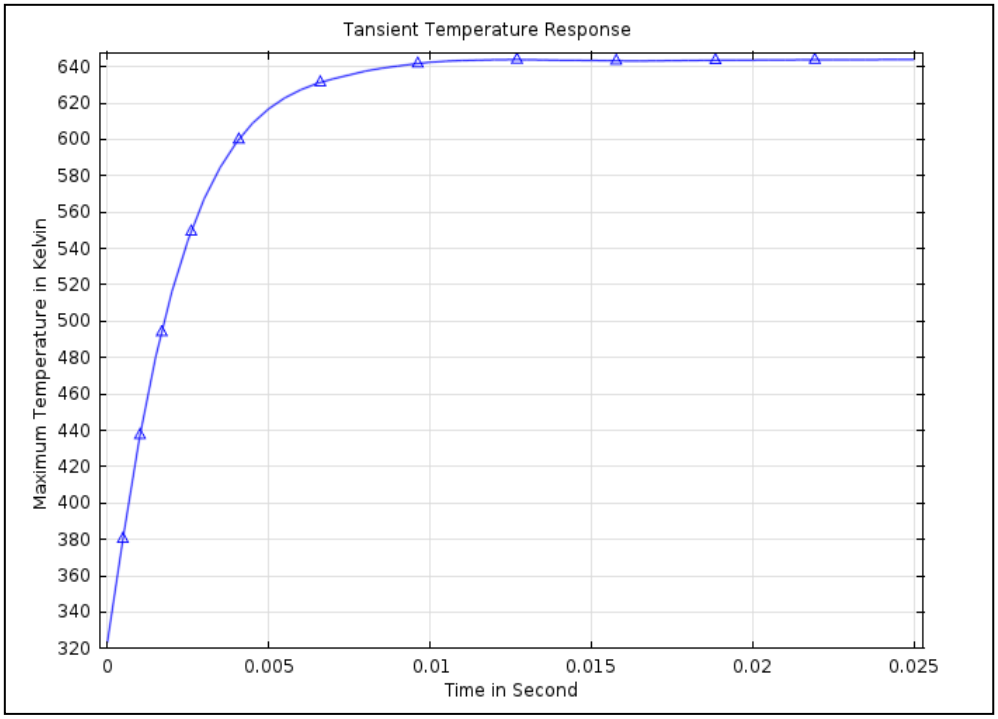

Fig. 5.5.7 Transient temperature response of Platinum based modified spiral geometry

Now we are changing width of micro-heater for better temperature uniformity as already seen in Fig. 5.4.6 and Fig. 5.4.7. And simulation result are analyzed for the same supply voltage of 0.3 V. Fig. 5.5.8 represents surface temperature response of Platinum based micro-heater.

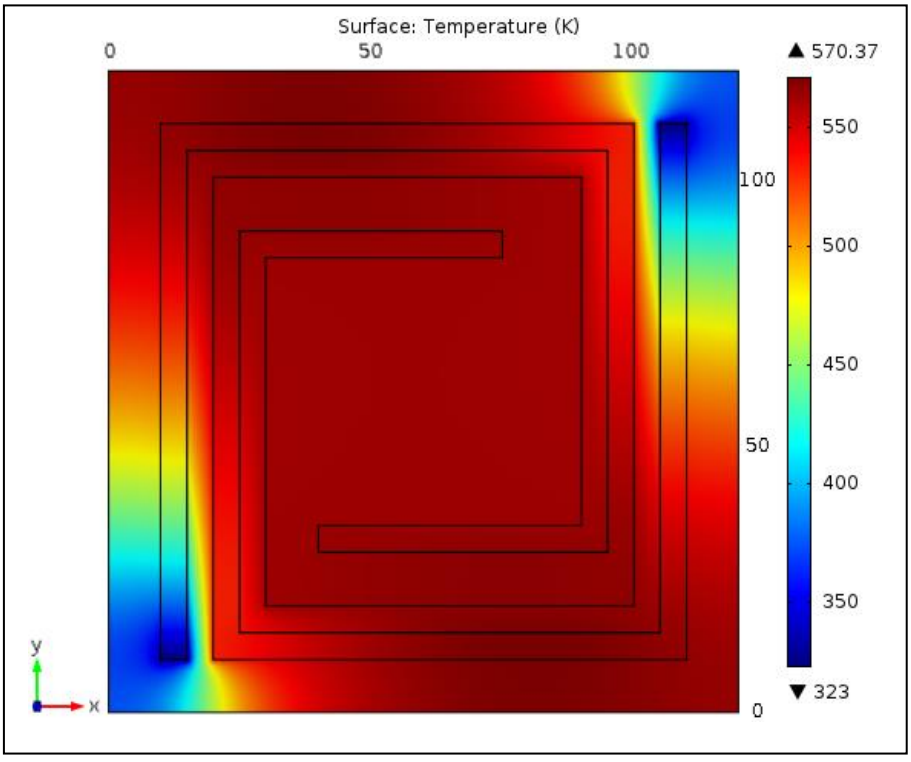

Fig. 5.5.8 Simulated Platinum based changed width micro-heater geometry

It can be observed that maximum surface temperature reduces from 645.47° K to 570.37° K. If we increase applied voltage from 0.3 V to 0.3555 V, we can achieve same 645.47° K. Now consider supply voltage of 0.3555 V then surface density is shown in Fig. 5.5.9. There is less current density at centre of micro-heater geometry.

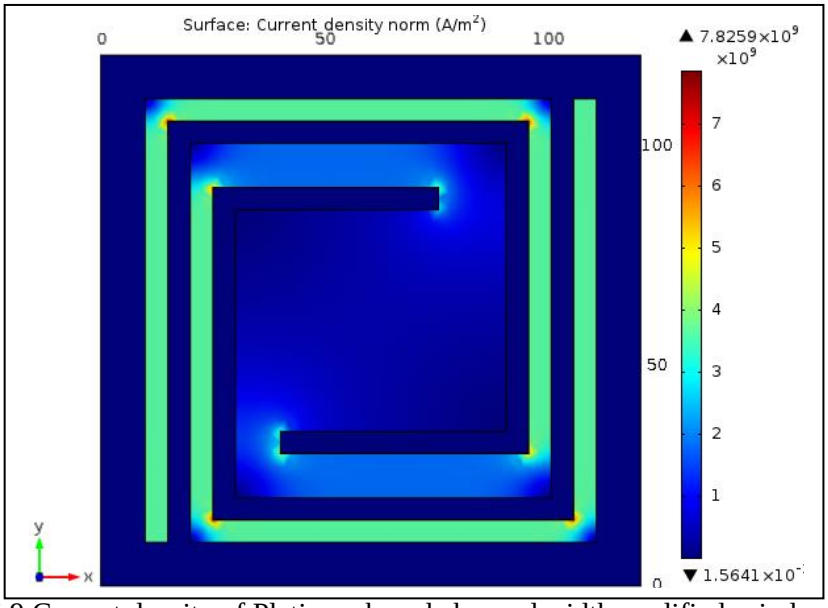

Fig. 5.5.9 Current density of Platinum based changed width modified spiral geometry

Also Fig. 5.5.10, Fig. 5.5.11 and Fig. 5.5.12 are represented by transient resistance response, transient power consumption response and transient temperature response respectively.

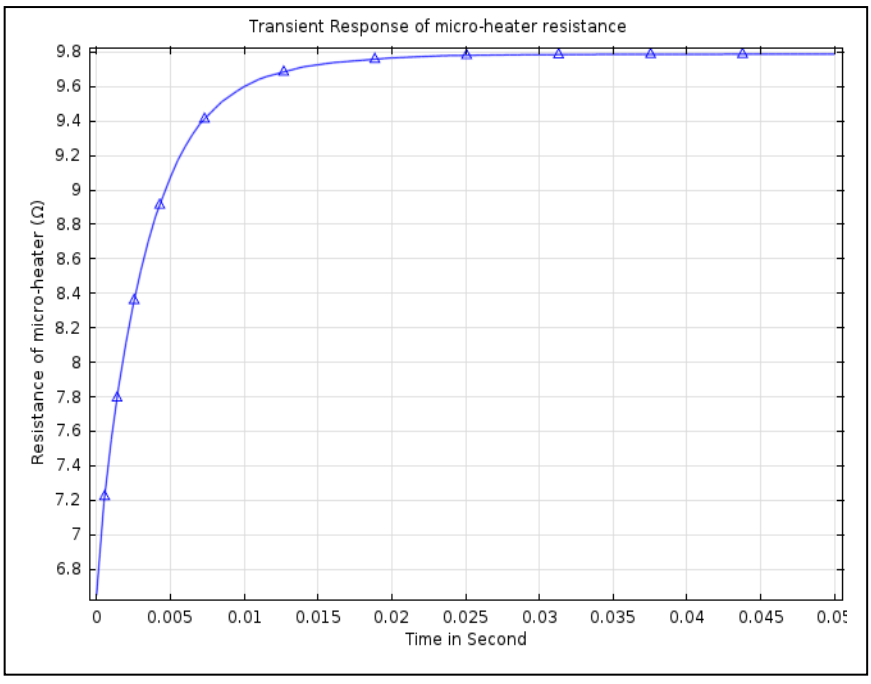

Fig. 5.5.10 Transient response of Platinum based changed width micro-heater resistance

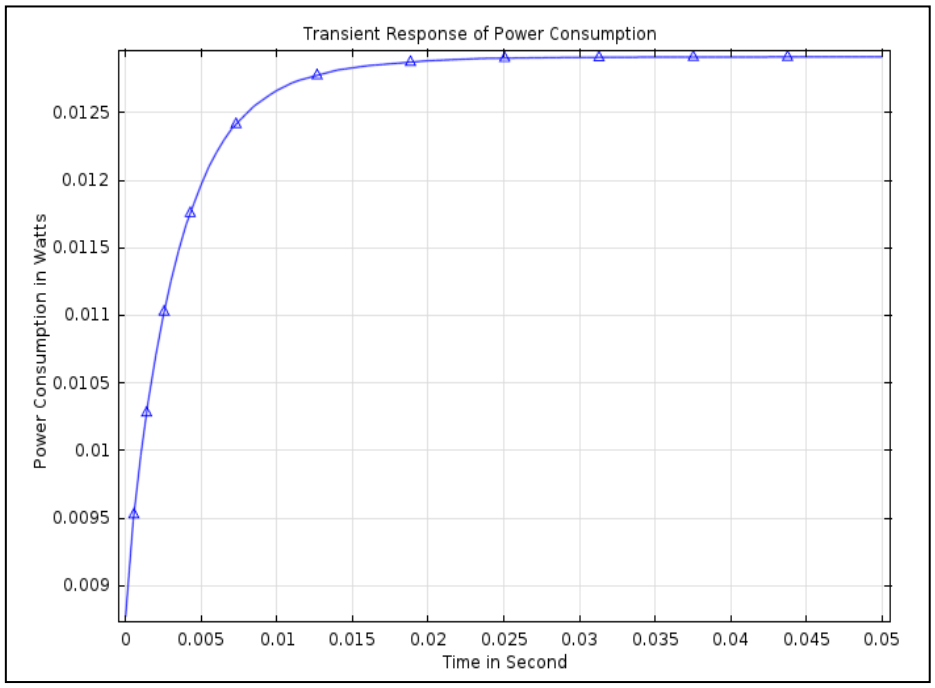

Fig. 5.5.11 Transient response of power consumption of Platinum based changed width modified spiral geometry

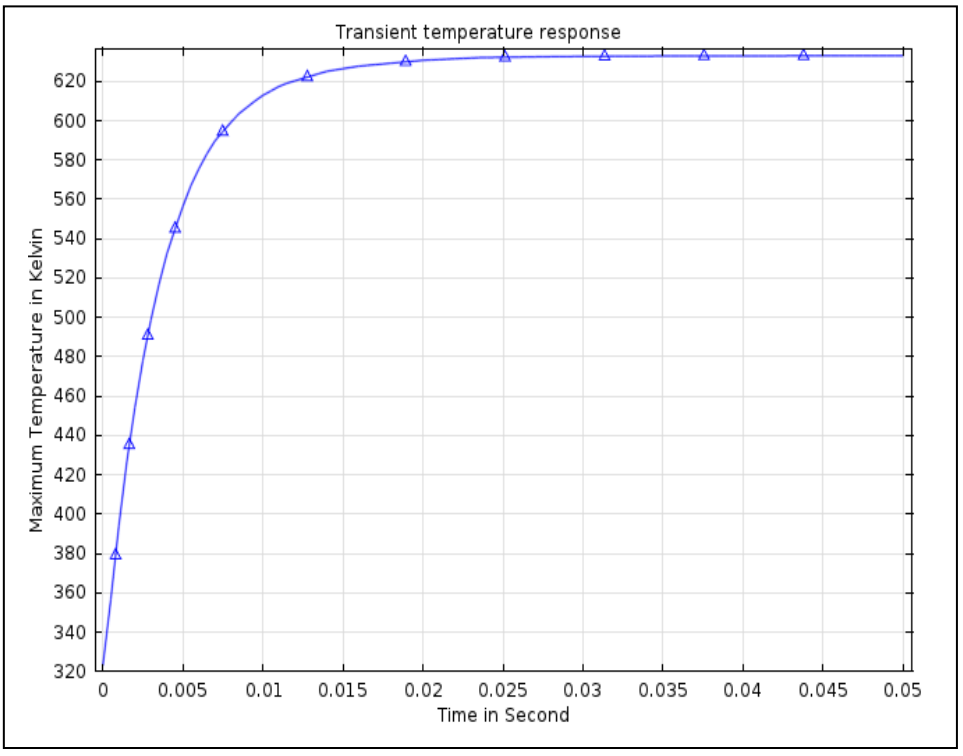

Fig. 5.5.12 Transient temperature response of Platinum based changed width modified spiral geometry

Results are compared for both the Platinum based geometries and shown in Table 5.5.2.

Table 5.5.2 Comparison of parameters of two geometries for Platinum

	Spiral Geometry with equal width of 10µm	**Spiral Geometry with unequal width**
Max. Surface Temperature	645.47 °K at 0.3 V	570.37° K at 0.3 V 645.47 °K at 0.3555 V
Transient Temperature response time	16.4 ms	27 ms
Resistance Variation	3.28 Ω to 4.8 Ω (till temperature reaches 323 °K to 645.47 °K)	6.6 Ω to 9.8 Ω (till temperature reaches 323 °K to 645.47 °K)
Power Consumption	18.83 mW	12.89 mW

Now, parameters comparison of Poly-Si and Platinum based modified spiral geometry covers in Table 5.5.3 and after changing width of modified spiral geometry are compared in Table 5.5.4.

Table 5.5.3 Parameters comparison of modified spiral geometry for Poly-Si and Platinum

	Poly-Si based modified Spiral geometry	**Platinum based modified Spiral geometry**
Max. Surface Temperature	645.47° K at 3.0 V	645.47° K at 0.3 V
Transient Temperature response time	13 ms	16.4 ms
Resistance Variation	600.51 Ω to 712.54 Ω (till temperature reaches 323 °K to 645.47 °K)	3.28 Ω to 4.8 Ω (till temperature reaches 323° K to 645.47° K)
Power Consumption	12.63mW	18.83 mW

Table 5.5.4 Comparison of parameters of modified spiral geometry with changed width for Poly-Si and Platinum

	Poly-Si based modified Spiral geometry	**Platinum based modified Spiral geometry**
Max. Surface Temperature	572.89 °K at 3.0V 645.47 °K at 3.4662V	570.37° K at 0.3 V 645.47 °K at 0.3555 V
Transient Temperature response time	23 ms	27 ms
Resistance Variation	1210.6 Ω to 1433.8 Ω (till temperature reaches 323 °K to 645.47 °K)	6.6 Ω to 9.8 Ω (till temperature reaches 323 °K to 645.47 °K)
Power Consumption	8.3791mW	12.89 mW

5.6 Conclusion

After simulation of Poly-Si and Platinum based geometry, it is clear that Platinum consumes more power and has more transient temperature response time to achieve same temperature which was attained by in Poly-Si based structure. While we need very less applied voltage in case of Platinum based micro-heater to reach same temperature value compare with Poly-Si based micro-heater geometry. Though there are some disadvantages in case of Poly-Si based micro-heater like, less temperature stability and fabrication difficulty. There are certain drawbacks in case of Platinum based micro-heater such as, more expensive and less resistivity.

CHAPTER-6

6.1 Fabrication steps of MEMS based gas sensor

For design of MEMS based gas sensor, Silicon <100> is used as substrate material shown in Fig. 6.1.

Fig. 6.1 Silicon wafer <100> as substrate

Its fabrication steps are as followed:

- Wafer cleaning
- Oxidation
- Lithography
- Platinum deposition
- Silicon nitride deposition (sputtering) and annealing
- Back side membrane patterning and Oxide Etching
- Silicon etching using TMAH solution
- Silicon nitride removal
- IDT deposition
- Deposition of Sensing layer

6.1.1 Wafer Cleaning

Generally, before using silicon wafer in fabrication process, it should be cleaned chemically to remove heavy metals, organic films and particulates. There are three different techniques available for cleaning.

- Piranha Cleaning
- RCA- 1 Cleaning
- RCA-2 Cleaning

For use any one technique, one should switch on the exhaust of chemical hood. Wear protective gown, goggle, mouth mask, head cap just before starting work on wet bench.

(A) Piranha Cleaning

Piranha solution which is used for cleaning purpose, is made of a mixture of H_2SO_4 (sulfuric acid) and H_2O_2 (hydrogen peroxide). As the mixture is a strong oxidizing agent, that will clean most of organic matter, also it will also hydroxylate partially all surfaces (add OH groups) and it is making them highly hydrophilic (water compatible).

There are many different mixture ratios utilized and all are commonly called piranha. A typical mixture is 3:1 concentrated H_2SO_4 (sulfuric acid) to 30% H_2O_2 (hydrogen peroxide); other protocols can be used a 4:1 or even 7:1 mixture. A closely related mixture, sometimes called "base piranha", is a 3:1 mixture of ammonium hydroxide (NH_4OH) with hydrogen peroxide. Piranha solution must be made with great precautions. It is very corrosive and also an extremely powerful oxidizer. Surfaces must be carefully cleaned, and totally free of organic solvents before coming into contact with piranha solution. Piranha solution makes clean by dissolving organic impurities, and a large amount of impurity will reason violent bubbling also a discharge of gas that can cause an explosion.

Piranha solution must be prepared by adding H_2O_2 (hydrogen peroxide) to H_2SO_4 (sulfuric acid) very slowly, never vice versa. This process will generate heat. The resultant heat can increase solution temperatures exceeding 100° C. Before applying any heat, it must be permissible to cool reasonably. The abrupt raise in temperature can also lead to violent boiling, or even spraying of the tremendously acidic solution. Explosions may occur if the peroxide solution concentration is higher than 50% of total solution. Once the mixture is become stable, it can be further heated to maintain its reactivity. The hot (often bubbling) solution will clean organic composites off substrates, and oxidize or hydroxylate most of surfaces. Cleaning usually requires about 10 to 40 minutes, after which time the substrates can be removed from the solution.

The solution may be mixed before application or directly applied to the material, applying the sulfuric acid first, followed by the peroxide. Due to the self-decomposition of hydrogen peroxide, piranha solution should be used freshly prepared. Piranha solution should not be stored. Immersing the substrate (such as a wafer) into the solution should be done slowly to prevent thermal shock that may crack the substrate material.

(B) RCA- 1 Cleaning

Take 2 quartz beakers, 1 measuring cylinder, wafer holder and wash with DI (Deionised) water. (DI water plant has been placed just next to the wet bench)

Preparation of RCA-1 solution:

RCA-1 is a solution of Deionised Water (DI H_2O): ammonium hydroxide (NH_4OH): H_2O_2 (hydrogen peroxide) (5:1:1)

(Always add reactive compounds (acid/base) to water)

a.) 200 ml DIH_2O

b.) 40 ml NH_4OH

c.) 40 ml H_2O_2

Take 200ml DI water into Cleaned beaker .Add 40ml H_2O_2 and 40ml NH_4OH to DI water. Once the solution is prepared, keep it on a hot plate. Turn on the hot plate and set temperature to 150° C. The solution will need to be heated to 80° C. This will take about 15 minutes. Once solution gets heated up to 80° C, load silicon wafer into wafer holder and immerse into heated RAC1 solution for 15 minutes. After 15 minutes of cleaning take out wafers from the solution and rinse with DI water thoroughly for 1minute.

(C) RCA- 2 Cleaning

Preparation of RCA-2 solution:

RCA-2 is a solution of Deionised Water (DI H_2O): Hydrochloric acid (HCl): H_2O_2 (hydrogen peroxide) (6:1:1)

a) 240 ml DI Water

b) 40 ml H_2O_2

c) 40 ml HCl

Take 240ml DI water into Cleaned beaker .First Add 40ml H_2O_2 and then 40ml HCl to DI water. Once the solution is prepared, keep it on a hot plate. Turn on the hot plate and set temperature to 150° C. The solution will need to heat to 80° C. This will take about 15 minutes. Once solution gets heated up to 80° C, load silicon wafer into wafer holder and immerse into heated RAC-2 solution for 15 minutes. After 15 minutes of cleaning take out wafers from the solution and rinse with DI water thoroughly for 1minute.

The RCA-2 cleaning removes metallic contaminants from the wafer.

Preparation of dilute HF (hydrofluoric acid solution):

Measure 200ml of DI water using measuring cylinder and pour into 250 ml polypropylene beaker and then measure 2ml of HF in a polypropylene measuring cylinder and add to DI water and mix thoroughly using Teflon rod. Then dip RCA2 cleaned silicon wafer into dilute HF solution for 15 seconds and finally rinse with DI water for 1min.
Now the wafers are ready for thermal wet oxidation process.

6.1.2 Oxidation

There are four different methods of oxidation as mentioned below:

1. Diffusion oxidation
2. Wet oxidation
3. High pressure oxidation
4. Plasma oxidation

Though all methods are effective but wet oxidation is used for MEMS based gas sensor fabrication process. Wet oxidation is explained with details as below.

Switch on the mains of thermal wet oxidation furnace to grow 1000 nm oxide layer. Ramp up furnace temperature to 500° C and pass nitrogen gas (0.5 liter/min) into the furnace to create inert nitrogen atmosphere. Then load the wafers into furnace and ramp up furnace temperature from 500° C to 1100° C. Now pass oxygen gas (1 liter/min) directly into the furnace for 10 minutes for dry oxidation. After 10 minutes stop direct supply of oxygen gas into the furnace and pass oxygen through the water bubbler (bubbler temperature should be 97° C) for 3hrs for wet oxidation. After 3hrs stop oxygen supply and pass nitrogen gas (0.5 liter/min).Ramp down the furnace temperature to 37° C and unload the wafers. This oxide is used as a hard mask during the Potassium Hydroxide (KOH) etching process. After this step, we have structure as shown in Fig. 6.2.

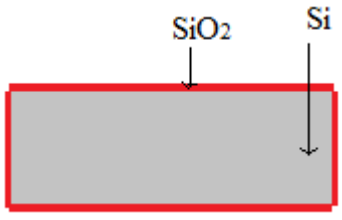

Fig. 6.1.2 Structure after wet oxidation

6.1.3 Lithography

Top side of oxidized wafer is coated with S1813 Photoresist at 4000rpm for 40secs and prebaked at 125° C temperature for 1minute for top layer pattern transferring double sided EVG 620 mask aligner was used. The UV bulb is switched on for 10 minute for stabilization. Mask is loaded according to procedure (guided by software on the screen)

The parameters set are:

Soft Contact

Constant Dosage - 75mJ/cm^2

Wafer is loaded and aligned with the mask

The mask pattern is transferred onto the coated photoresist by UV exposure

The pattern is then developed in a MF26A developer solution for 1min and rinsed with DI water followed by nitrogen drying.

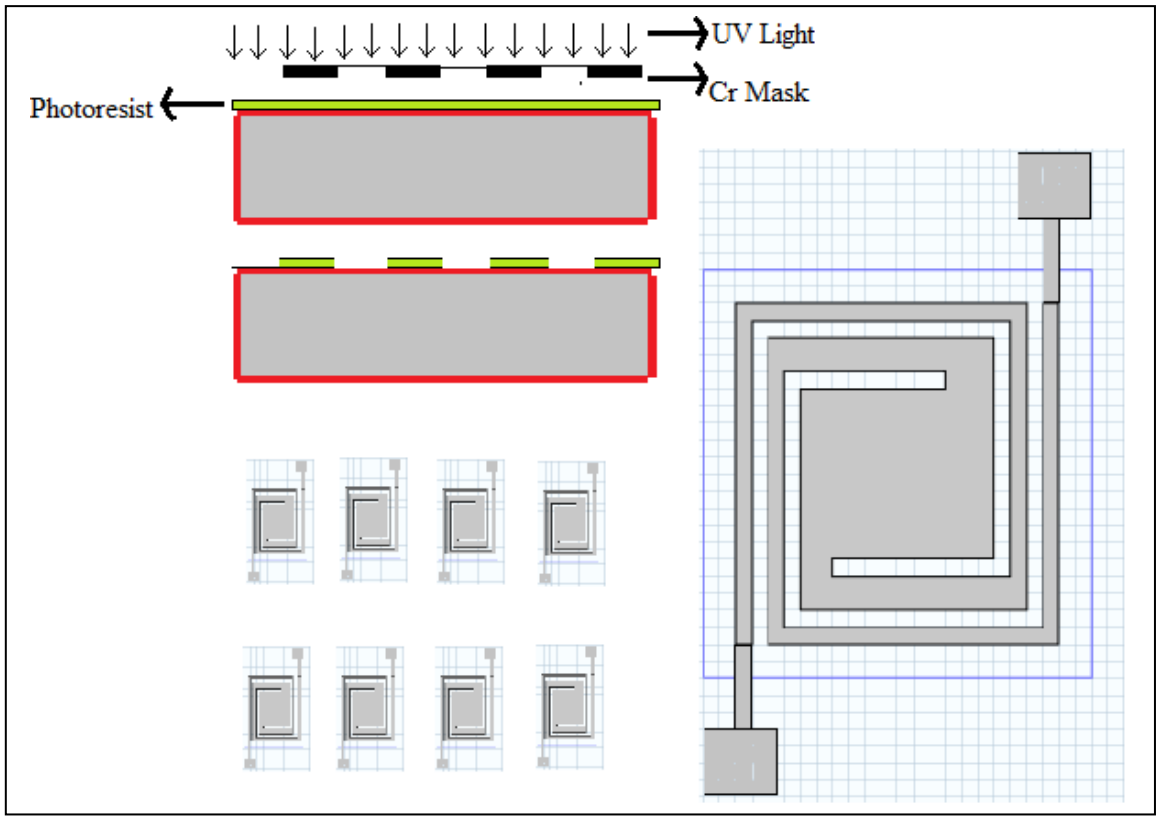

6.1.3 Top view of mask lay out design of micro-heater with dimension

6.1.4 Platinum deposition

200nm platinum was deposited after lithography process by sputtering method.

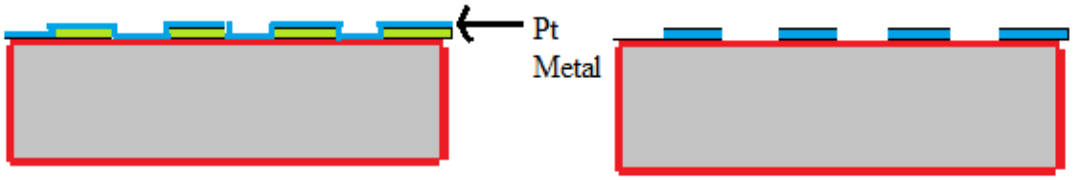

Fig. 6.1.4 Structure after Platinum deposition

Sputtering parameters:

Plate voltage: 1.5 KV

Incident power: 60w

Reflected power: 25w

Plate current: 60mA

Distance between target and substrate: 5.2cm

Pre sputtering time: 2min

Deposition time: 8min

6.1.5 Silicon nitride deposition (sputtering) and annealing

80nm silicon nitride was deposited as a hard mask for bulk silicon etching.

Sputtering parameters:

Plate voltage: 1.5KV

Incident power: 60W

Reflected power: 20W

Plate current: 60mA

Distance between target and substrate: 6cm

Pre sputtering time: 15min

Deposition time: 15min

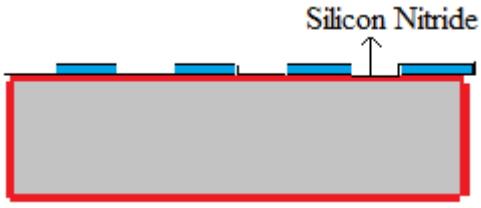

Fig. 6.1.5 Structure after Silicon Nitride deposition

After deposition nitride was annealed in a polymer annealing furnace at 700° C temp for 45 min in nitrogen ambient. Flow rate of nitrogen was 0.5 ltr/min.

6.1.6 Back side membrane patterning and Oxide Etching

Back side of oxidized wafer was coated with S1813 Photoresist at 4000rpm for 40secs and prebaked at 125 degree temp for 1min.For membrane pattern was aligned with respect to top layer pattern by double sided EVG 620 mask aligner.

The UV bulb is switched on for 10 min for stabilization.

Mask is loaded according to procedure (guided by software on the screen)

The parameters set are:

Soft Contact

Constant Dosage - 75mJ/cm2

Wafer is loaded and aligned with the mask

The mask pattern is transferred onto the coated photoresist by UV exposure. The pattern is then developed in a MF26A developer solution for 1min and rinsed with DI water followed by nitrogen drying.

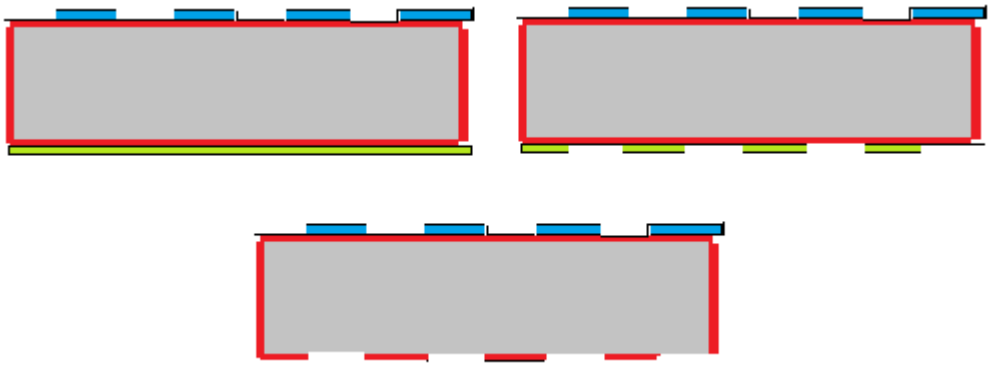

Fig. 6.1.6 Structure after membrane patterning and Oxide Etching

6.1.7 Silicon etching using KOH + IPA and TMAH solution

Preparation of 30% KOH solution:

Weigh 105g of 85% pure KOH pellets into 250ml glass beaker and add 195ml of DI water and stir it thoroughly till KOH pellets dissolves completely. Keep this solution on a hot plate for heating to 75° C .once after reaching temperature add 50ml of IPA to the heated KOH solution and immerse wafer into the solution for silicon etching for 2hrs and 30min after 2hrs and 30min etching take out wafer from the solution and wash with DI water thoroughly and dry with nitrogen.

Etch rate of silicon in KOH+IPA is 50micron/ hour and etch rate of silicon oxide is 150nm / hour.

Preparation of 5% TMAH solution:

Take 200ml of DI water in a clean 250ml beaker and then add 40ml of 25%TMAH solution. Once the solution is prepared, keep it on a hot plate .Turn on the hot plate and set temperature to 150° C. The solution will need to heat to 75° C. This will take about 15 minutes. Once solution gets heated up to 75° C, add 0.2g of ammonium persulphate salt to the solution. Load KOH+IPA etched silicon wafer into wafer holder and immerse into heated TMAH solution for 3 hrs for further silicon etching. Take out sample from the solution and rinse with DI water followed by methanol.

(Ammonium persulphate should be added at each 15 minutes interval during etching).

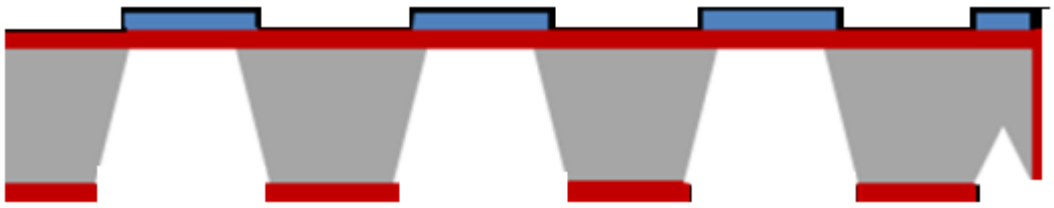

Fig. 6.1.7 Structure after Silicon etching using KOH + IPA and TMAH solution

6.1.8 Silicon Nitride Removal

Silicon nitride was etched using 1:3 BHF solution by dipping for 10secs.After etching of silicon nitride layer wafer was thoroughly rinsed with DI water and dried with nitrogen.

Fig. 6.1.8 Structure after removal of Silicon Nitride

6.1.9 IDT deposition

For deposition of IDT (Interdigitated Electrodes), there is same procedure followed which is used in micro-heater deposition. Generally, Au or/and Ag materials are used for IDT. Use of IDT is to detect resistance change of sensing surface.

Fig. 6.1.9 IDT structure for detection of resistance change of sensing surface

6.1.10 Deposition of Sensing Layer

On IDT electrodes, sensing surface is deposited. Typically, Tin oxide (SnO_2), Zinc oxide (ZnO), Tungsten trioxide (WO_3), Indium tin oxide (ITO), Titanium oxide (TiO_2), Cerium oxide (CeO_2) are used for sensing surface.

CHAPTER-7

7.1 Conclusion

In this micro-heater for MEMS based metal oxide gas sensor has been studied in details. Principle of joule-heating has discussed to understand the working of micro-heater. Design criteria and design rules have been provided by research methodology and obtained results for better analysis and better optimization of gas sensor with satisfying some basic requirements such as, low power consumption, better temperature uniformity and transient temperature response time with low risk of break and burn through. Different micro-heater geometries are designed and simulated for finding best suitable option for gas sensor application. Dimensions of geometry have been varied to achieve better temperature uniformity. Their characteristics such as power consumption, surface temperature response, transient resistance response, current density distribution and transient temperature response time have been studied in details and results are compared. In Chapter 6, fabrication steps are discussed for implementation of MEMS based metal oxide gas sensor.

Among the various micro-heater geometries, modified spiral geometry has been chosen for analysis as it provides better temperature uniformity in all available micro-heater geometries. Poly-Si and Platinum are the materials used for design and simulation of micro-heater. Poly-Si and Platinum based micro-heater are analyzed to achieve 640 - 650^o K temperature. Poly-Si based micro-heater has achieved this temperature at 3.0 V applied voltage. Its resistance variation was from 600.51 Ω to 712.54 Ω (till temperature reaches 323° K to 645.47° K) with transient temperature response time of around 13 ms. Also power consumption is around 12.63 mW. While in case of Platinum based micro-heater 640 - 650^o K temperature range has been achieved at applied voltage of 0.3 V only. Variation of resistance is from 3.28 Ω to 4.8 Ω (till temperature reaches 323° K to

645.47° K) with transient temperature response time of 16.4 ms. And Power consumption is of 18.83 mW in case of Platinum based micro-heater.

So After simulation of Poly-Si and Platinum based geometry, it is clear that Platinum consumes more power and has more transient temperature response time to achieve same temperature which was attained by in Poly-Si based structure. While we need very less applied voltage in case of Platinum based micro-heater to reach same temperature value as of Poly-Si based micro-heater geometry. Though there are some disadvantages in case of Poly-Si based micro-heater like, less temperature stability and fabrication difficulty. There are certain drawbacks in case of Platinum based micro-heater such as, more expensive and less resistivity.

7.2 Future Scope

In future more optimization is possible to make better micro-heater geometry. As different applications need different micro-heaters, it is more crucial part of micro-heater design to optimize parameters and to select proper material. Design parameter optimization can be achieved by varying substrate thickness, dimensions and modification of micro-heater internal edges. Recently, Dilver P1 (which is composition of alloy like, Fe, Ni and Co) is considered available option as it consumes less power and having good resistivity though it generates less temperature compared to Platinum and Poly-Si.

REFERENCE:

[1] M. Mehregany, "Microelectromechanical syatem", *Circuit and Devices Magazine IEEE*, vol. 9, no. 6, pp. 14-22, July 1993.

[2] Stephen D. Senturia, *Microsystem Design*. London: Kluwer Academic Publishers, November 2000.

[3] *"What is MEMS Technology?,"* www.mems-exchange.org [Online]. Available: https://www.mems-exchange.org/MEMS/what-is.html, [Accessed: 2 June 2014].

[4] *An Introduction to MEMS*, PRIME Faraday Partnership, Loughborough University, Loughborough, U.K., 2003.

[5] Zaini Abdul Halim, "Design of Microhotplate Based Gas Sensing System", *Ph.D Thesis*, Electrical & Electronic Engineering Department, Universiti Sains Malaysia, May 2008.

[6] R. Ghodssi and P. Lin, "*MEMS Materials and Processes Handbook*", Springer, New York, London, 2011.

[7] K. Arshak, E. Moore, G.M. Lyons, J. Harris and S. Clifford, "A review of gas sensors employed in electronic nose applications". *Sensor Review*, vol. 24, no. 2, pp.181-198, November, 2004.

[8] T.C. Pearce, S. S. Schiffman, H.T. Nagle, and J. W. Gardner, *Handbook of Machine Olfaction*, Wiley-VCH, Weinheim, 2003.

[9] Frank Ro¨ck, Nicolae Barsan, and Udo Weimar, "Electronic Nose: Current Status and Future Trends". *Chemical Reviewer*, vol. 108, pp. 705-725, August 2008.

[10] Fauzan Khairi Che Harun, Andik Marwintan Jumadi and Nasrul Humaimi Mahmood, "Carbon black polymer composite gas sensor for electronic nose", *International Journal of Scientific & Engineering Research*, vol. 2, no. 11, November 2011.

[11] Alphus D. Wilson 1, and Manuela Baietto, "Applications and Advances in Electronic-Nose Technologies", *Sensors*, vol.9, pp. 5099-5148, June 2009.

[12] Seokheun Choi, Simeng Chen, Yuchao Wang, " Applications and Technology of Electronic Nose for Clinical Diagnosis", *Open Journal of Applied Biosensor*, vol. 2, pp. 39-50, May 2013.

[13] Paul E. Keller, Lars J. Kangas, Lars H. Liden, Sherif Hashem, Richard T. Kouzes, "Electronic noses and their applications", *Proceedings of IEEE Northcon/Technical Applications Conference (TAC'95),* Portland, OR, USA, 12 October 1995.

[14] J. W. Gardner, E. L. Hines, and M. Wilkinson, *"*Application of Artificial Neural Networks to an Electronic Olfactory System*", Measurement Science and Technology*, vol. 1, pp. 446-451, November 1990.

[15] David Tin Win, "The Electronic Nose – A Big Part of Our Future", *AU J.T.*, vol. 9, no. 1, pp. 1-8, July 2005.

[16] K. Wetchakuna, T. Samerjaia, N. Tamaekonga, C. Liewhirana, C. Siriwonga, V. Kruefua, A. Wisitsoraatb, A. Tuantranontb and S. Phanichphanta, "Semiconducting metal oxides as sensors for environmentally hazardous gases.", *Sensors and Actuators B*, vol.160, pp. 580– 591, August 2011.

[17] George Preti, Thomas S. Gittelman, Paul B. Staudte, and Preston Luitweiler, "Letting the nose lead the way: malodorous components in drinking water", *Analytical Chemistry*, vol. 65, no. 15, pp. 699A-702A, August 1993.

[18] T.V. Belysheva, L.P. Bogovtseva, E.A. Kazachkov and N.V. Serebryakova, "Gas-sensing properties of doped In_2O_3 films as sensors for NO_2 in air", *Journal of Analytical Chem*estry, vol. 58, no. 6, pp. 583–587, 2003.

[19] Kane Jonathan Miller, "Simulation and fabrication of microhotplates for metal oxide gas sensors", *M.Tech Dissertation*, Chemical Department, B.S. University of Louisville, August 2010.

[20] Kraig D. Mitzner, Jason Sternhage and David W. Galipeau, "Development of a micromachined hazardous gas sensor array", *Sensors and Actuators B*, vol. 93, pp.92-99, 2003.

[21] Tetsuro Seiyama, Akio Keto, Kiyoshi Jiishi and Masonori Nagatani, "A New Detector for Gaseous Components Using Semiconductive Thin Films", *Analytical Chemistry*, vol. 34, no.11**,** pp.1502-1503, October 1962.

[22] H. Meixner and U. Lampe, "Metal oxide sensors", *Sensors and Actuators B,* vol. 33, pp. 198-202, February 1996.

[23] Martin Hausner, Johannes Zacheja and Josef Binder, "Multi-electrode substrate for selectivity enhancement in air monitoring", *Sensors and Actuators B,* vol. 43, pp. 11–17, April 1997.

[24] Marius Dumitrescu, Cornel Cobianu, Dan Lungu, Dan Dascalu, Adrian Pascu, Spas Kolev and Albert van den Berg, "Thermal simulation of surface Micromachined polysilicon hotplates of low power consumption", *IEEE*, pp. 83-86, 1998.

[25] S. Semancik, R.E. Cavicchi, M.C. Wheeler, J.E. Tiffani, G.E. Poierier, R.M. Walton, J.S. Suehle, B. Panchapakesan and D.L. De Voe, "Microhotplate platforms for chemical sensor research", *Sensors and Actuators B*, vol. 77, pp. 579–591, 2001.

[26] Isolde Simon, Nicolae BaÃrsan, Michael Bauer and Udo Weimar, "Micromachined metal oxide gas sensors: opportunities to improve sensor performance", *Sensors and Actuators B,* vol. 73, pp. 1-26, 2001.

[27] M. Afridi, A. Hefner, D. Berning, C. Ellenwood, A. Varma, B. Jacob and S. Semancik, "MEMS-based embedded sensor virtual components for system-on-a-chip (SoC)", *Solid-State Electronics*, vol. 48, pp. 1777–1781, 2004.

[28] M. Baroncini, P. Placidi, G.C. Cardinali and A. Scorzoni, "Thermal characterization of a microheater for micromachined gas sensors", *Sensors and Actuators A*, vol. 115, pp. 8–14, 2004.

[29] J. Cerdà Belmonte, J. Puigcorbe, J. Arbiol , A.Vila, J. R. Morante, N. Sabate, I. Gracia and C. Cane," High-temperature low-power performing micro machined suspended micro-hotplate for gas sensing applications". *Sensors and Actuators B,* vol. 114, pp. 826–835, 2006.

[30] Ching-Liang Dai, Mao-Chen Liu, Fu-Song Chen, Chyan-Chyi Wu and Ming-Wei Chang, "A nanowire WO_3 humidity sensor integrated with micro-heater and inverting amplifier circuit on chip manufactured using CMOS-MEMS technique", *Sensors and Actuators B,* vol. 123, pp. 896–901, 2007.

[31] J. F. Creemer, D. Briand, H. W. Zandbergen, W. van der Vlist, C. R. de Boer, N. F. de Rooij and P. M. Sarro,"Microhotplates with TiN heaters", *Sensors and Actuators A,* vol. 148, pp. 416–421, 2008.

[32] H. Y. Lee, S. Moon, S. J. Park, J. Lee, K.-H. Park and J. Kim, "Micro- Machined resistive micro-heaters for high temperature gas sensing applications", *Electronics Letters,* vol. 44, no. 25, 2008.

[33] G. Velmathi, N. Ramshanker and S. Mohan, "2D Simulations and Electro-Thermal Analysis of Micro-Heater Designs Using COMSOLTM for Gas Sensor Applications", in *Proceedings of the COMSOL Conference*, India, 2010.

[34] Jae-Cheol Shim and Gwiy-Sang Chung, "Fabrication and Characteristics of Pt/ZnO NO Sensor Integrated SiC Micro Heater", in *Proceedings of IEEE SENSORS Conference,* pp. 350-353, 2010.

[35] M. Gayake, D. Bokdas and S. Gangal, "Simulations of Polymer based Microheater Operated at Low Voltage", in *Proceedings of the COMSOL Conference*, Bangalore, India, 2011.

[36] Vineet Bansal , Anil Gurjar, Dinesh Kumar and B. Prasad, "3-D Design, Electro-Thermal Simulation and Geometrical Optimization of spiral Platinum Micro-heaters for Low Power Gas sensing applications using COMSOL^{TM}", in *Proceedings of the COMSOL Conference*, India, 2011.

[37] Susmita Sinha, Sunipa Roy and C. K. Sarkar, "Design & Electro-Thermal Analysis of Microheater for Low Temperature MEMS based Gas Sensor", in *Proceedings of Chennai and Dr.MGR University Second International Conference on Sustainable Energy and Intelligent System (SEISCON 2011)* , Dr. M.G.R. University, Maduravoyal, Chennai, Tamil Nadu, India, pp. 20-22, July 2011.

[38] Bijoy kantha, Pallavi kar, Saral saha and Subir Kumar sarkar, "Design and Electro-Thermal Analysis of MEMS based Micro-hotplate for Gas Sensor", *Chennai and Dr. MGR University Second International Conference on Sustainable Energy and Intelligent System,* 2011.

[39] L. Sujatha, V. S. Selvakumar, S. Aravind, R. Padamapriya and B. Preethi, "Design and Analysis of Micro-Heaters using COMSOL Multiphysics for MEMS Based Gas Sensor", *Proceedings COMSOL Conference*, India, 2012.

[40] Jianhai Sun, Dafu Cui, Lulu Zhang, Xing Chen, Haoyuan Cai and Hui Li, "Fabrication and characterization of a double-heater based MEMS thermal flow sensor", *Sensors and Actuators A*, vol. 193, pp. 25– 29, 2013.

[41] *Introduction to COMSOL Multiphysics users manual*, Oct. 2012

[42] Chris Long & Naser Sayma, "Heat Transfer Module", Venture Publishing AsP, 2009.

[43] *Introduction to Structural Mechanics Module users manuals*, May 2012.

[44] S. M. Lee, D.C. Dyer and J. W. Gardner, "Design and optimization of a high-temperature silicon micro-hotplate for nanoporous palladium pellistors", *Microelectronics Journal*, vol. 34, pp.115–126, 2003.

[45] Lie-yi Sheng, Zhenan Tang, Jian Wu, Philip C.H. Chan and Johnny K.O. Sin, "A low-power CMOS compatible integrated gas sensor using maskless tin oxide sputtering", *Sensors and Actuators B*, vol. 49, pp. 81–87, 1998

[46] Indrajit Singh and S. Mohan, "3D simulation and elecro-thermal analysis of micro-hotplate design using CoventorWare for MEMS based gas sensor application", *International conference on smart material structures and systems*, pp. 28-30, 2005.

[47] J. Jakovenkoa, T. Lalinsky, M. Drzik, M. Ivanova, G. Vankob and M. Husak, "GaN, GaAs and Silicon based Micromechanical Free Standing Hot Plates for Gas Sensors", Chemistry 1, pp. 804–807, 2009.

[48] V. K. Khanna, Mahanth Prasad, V. K. Dwivedi, Chandra Sekhar, A. C. Pankaj and J. Basu, "Design and Electro-Thermal Simulation of a Polysilicon micro-heater on suspended membrane for use in gas sensing", *Indian Journal of Pure and Applied Physics*, vol. 45, pp. 332-335, April 2007.

APPENDIX-I

Material properties used in simulation

Sr. No.	Properties	SiO_2	Poly-Si	Platinum
1.	Co efficient of thermal expansion in 1/K	0.5e-6	2.6e6	8.80e6
2.	Heat capacity at constant pressure in J/kg-K	730	678	133
3.	Relative permittivity	4.2	4.5	7.0
4.	Density in kg/m^3	2200	2320	21450
5.	Thermal Conductivity in W/m-K	1.4	34	71.6
6.	Young's modulus in Pa	70e9	160e9	168e9
7.	Poisson's ratio	0.17	0.22	0.38
8.	Electrical Resistivity in Ω-m	10e18	0.00002	10.6e-8

LIST OF PUBLICATION

Published:

[1] Palak Bhatt and Anil Arora, "Area effect analysis on surface temperature gradient in MEMS micro heater for gas sensor applications", in *Proceeding International Conference on Emerging Technologies in Electronics & Communication (ICETEC-13),* pp. 117-119, Dec. 20-22, 2013.

[2] Palak Bhatt, Manish Deshwal, H. Monga and Anil Arora, "Uniform Temperature Distribution of MEMS Micro-heater for Efficient MEMS based Gas Sensors", in *Proceeding 3rd National Conference on Advances in Metrology (AdMet – 2014),* Feb. 19-21, 2014.

Communicated:

[1] Palak Bhatt, Himanshu Monga and Anil Arora, "Design and performance analysis of MEMS micro-heater for uniform temperature platform", *International Journal of Electronics,* June, 2014.